STATIC AND DYNAMIC FINITE
ELEMENT ANALYSIS OF
UNDERGROUND CAVITIES WITH
SOME REFERENCE TO NUCLEAR
REACTOR CONTAINMENTS

SAYED ABO ELFETOH SHEHA

STATIC AND DYNAMIC FINITE ELEMENT ANALYSIS OF

UNDERGROUND CAVITIES WITH SOME REFERENCE

TO NUCLEAR REACTOR CONTAINMENTS

by

©   Sayed Abo Elfetoh Sheha, B.Sc.

A Thesis submitted in partial fulfillment
of the requirements for the degree of
Master of Engineering

Faculty of Engineering and Applied Science
Memorial University of Newfoundland

August 1975

St. John's   Newfoundland

To my mother and to my father

ACKNOWLEDGEMENTS

ABSTRACT

The finite element method is used to study the static and dynamic behaviour of underground cavities in rock. The static loads are those resulting from the assumed free field initial stress state (in-situ state of stress) along with the deadweight of the rock. The dynamic loading is a constant step pulse resulting from a blast excitation. Temperature gradients that can follow an unexpected accident are also taken into consideration. In the range of loads applied, the rock is considered homogeneous, isotropic and linearly elastic. Cracks due to high tensile stresses are not allowed and rock sliding or joints are assumed not to exist. The effects of different types of liners such as reinforced concrete, prestressed concrete, steel plate liners, as well as active and passive rock bolting, on the stress patterns in the rock media and the liner are investigated.

An available computer programme is modified to take into account all the variables needed for the analysis including different configuration shapes. The modified programme can deal with initial stress or initial strain states which facilitates the simulation of in-situ stress or expansions due to temperature. The initial stresses, when specified in the bar elements, allow representation of prestress in the cases of the prestressed liner and active rock bolting. As the original programme dealt with dynamic loading only, the modifications include adaptation to static loading.

For preliminary design, the dynamic loading can be reasonably

substituted by stepping up the static loading defined by the peak value by a dynamic load factor ranging between 1.15 and 1.25. However, a finite element time history analysis should be carried out for the final design. A safety factor is required to take into account thermal stresses depending on the probability of occurrence of temperature rise inside the cavity.

Active rock bolting is found to be better than other kinds of reinforcement. Results obtained from the prestressed concrete liner are not reasonable indicating the need for further studies for modifying the tendon profile and other parameters.

TABLE OF CONTENTS

LIST OF TABLES

LIST OF FIGURES

CHAPTER 1

INTRODUCTION

1.1 General

The state of stress around underground openings has been the subject of many current investigations in view of the many practical engineering applications in mining, transportation and energy industries. Power reactor containments are of particular interest to this study. Although underground locations in rock are recommended, the experience in mining and transportation fields suggests deep soil locations as feasible alternatives.

Underground structures in rock or soil are in a state of static stress due to (i) the weight of the overlying material, and (ii) the historically induced stresses which remain in the rock. A dynamic disturbance propagating through the medium changes the stress pattern. The stresses due to interaction with the dynamic disturbance should be superposed on the existing static values to obtain the complete stress picture.

1.2 Scope of this Thesis

The finite element method is employed to study the interaction of a plane wave with underground lined openings in rock media. Static stresses due to the in-situ state of stress including the deadweight of the rock are also studied. The work includes the effect of different types of liners such as reinforced concrete, prestressed concrete, active and passive rock bolts and steel plate liners on the stress patterns. A study of thermal stress distribution is also included. A computer programme,

1

modified to study these cases, can now handle many new practical problems.

1.3 Outline of the Thesis

In Chapter I, the general description of the problem is presented. Chapter II reviews the literature with particular reference to rock bolting and prestressed concrete liners. In Chapter III, the finite element formulation for the different cases studies is explained. These include consideration of in-situ stresses, thermal stresses, prestressing and rock bolting. Criteria for finite element modelling in rock are also discussed. Chapter IV gives a detailed account of the computer programme used. Some problems to check the correctness of the programme are presented and followed by a flow-chart for the main steps of the programme. In Chapter V illustrative examples are presented with graphs of the effects of different variables on the stress patterns. Conclusions drawn from this study are listed at this chapter with recommendations for further study.

1.4 Notation

A	area of cross section
$[C]$	damping matrix
C_c	critical damping
C_p	compressional wave velocity
C_s	shear wave velocity
$[D]$	elasticity matrix
E	Young's modulus
F	applied force
$[K]$	global stiffness matrix
$[K_e]$	element stiffness matrix
L	length of member

$[M]$	lumped mass matrix for the structure
$[M_e]$	lumped mass matrix for an element
$\{P\}$	matrix of external forces
p	load intensity
$[R]$	transformation matrix
T	natural period of vibration
t	time index
U	horizontal displacement
ω	natural frequency
σ_h	horizontal stress
σ_v	vertical stress
σ_r	radial stress
σ_t	tangential stress
ν	Poisson's ratio
ρ	mass density
γ	weight density
δ	deflection
ζ	damping ratio
$\{\mathcal{E}\}$	element strain matrix

Other symbols are defined as they occur.

CHAPTER II

LITERATURE REVIEW

2.1. Stress and Deformation Properties of Rocks

The stress conditions in rock are basically different from those in soils or in younger sediments. Whereas in soils vertical stresses predominate and can be related directly to the weight of the overlying layers and lateral pressures are lower in accordance with Poisson's ratio, in rocks the stresses result from gravity and historically induced stresses such as tectonics, ice loading, and remnant stresses from erosion of overlying material; at very great depths, the stresses are of a hydrostatic nature. Faulting and inclined bedding of stratified rocks result in the development of inclined stresses.

Deformation properties of rock cannot be investigated, in general, according to the simplifying assumptions commonly used for metals. Rock deformations cannot be described by a single parameter in view of anisotropy and dependence of deformations on the magnitude and duration of the acting forces. Plasticity plays an important role in deformation.

2.2 In-situ Stresses of Rock Masses

The stresses which exist in virgin rock before excavation are called in-situ stresses or residual stresses. According to Heim's hypothesis (11), the residual stresses have a geological origin, a view to some extent confirmed by the fact that very large masses of rock show horizontal stress components to be much greater than the vertical stress components (Fig. 2.1). Assuming the vertical stress component σ_v to be

4

proportional to the weight of the rock overburden, the horizontal component σ_h is, most probably, of the same magnitude as the vertical component due to creep of the rock.

Terzaghi (30) used elasticity theory to point out that if rock is strained in the vertical direction by its own weight, its Poisson effect in the horizontal direction is restrained at great depths by the neighbouring masses of rock and creates horizontal stresses opposing the lateral expansion. This gives horizontal stresses less than the vertical, an explanation different from Heim's hypothesis.

A third explanation which supports Heim's hypothesis states that in static rock masses there is a tendency for shear stresses to be progressively relieved giving a hydrostatic stress distribution (assumption of zero shear), with the horizontal components equal to the vertical.

Work in the field of rock mechanics which includes the measurement of both relatively deep and near surface stress fields show that neither Heim nor Terzaghi are wholly correct in their theories regarding stresses. The state of stress may be within or outside the predicted stresses given by these theories, in fact it is very rare when a theoretical generalization can be used to predict stresses at a particular geological location in rock.

2.3 Induced Stresses

Experience has shown that shortly after excavation of a gallery in pressurized rock the surrounding rock shows signs of being strained. Rock bursts occur and deformations are observed. Interpretation of these rock deformations depends on the basic approach to the general state of residual stresses in rock masses.

Based on Heim's hypothesis, $\sigma_h = \sigma_v = p$ \hfill (2.1)

Each case of loading σ_h or σ_v will produce two stresses at the boundary, σ_r and σ_t. By the classical theory of elasticity one can get stress σ_t

by superposing the solution due to the two cases σ_h and σ_v. The resulting tangential stress is, $\sigma_t = 2p$ (2.2)

Whenever this tangential stress at a radius r from the centre of the cavity reaches the elastic limit of the rock material, plastic deformation will take place in the rock with small inward displacements. This leads to stabilization of the rock and the tunnel (Fig. 2.2). Jaeger (11) referred to another explanation given by Rabcewicz for the problem of induced stresses in rock based on the assumption that the gallery excavated in rock is subjected to a vertical stress $\sigma_v = p$ with $\sigma_h = 0$. At first wedge-shaped bodies on either sides of the cavity shear off and move towards the cavity in the horizontal direction (Fig. 2.3a) and lateral pressure is developed that causes the rock to move horizontally (Fig. 2.3b). In the next stage (Fig. 2.3c) the movement is increased and the rock buckles under continuous lateral pressure. Squeezing pressures (the last stage) are encountered in mining, if the rock is of a poor nature.

2.4 Stress Analysis of Single Openings

The common practice for stress analysis of openings in rock is to use elastic theory. This includes certain simplifying assumptions regarding mechanical properties of rock, shape of the opening and the stress field. Generally all analysis is restricted to two-dimensional plane strain and mathematical solutions are available only for simple shapes that can be expressed by mathematical expressions such as circles or ellipsoids. Three types of stress fields commonly considered are shown in Fig. 2.4. Application of the finite element technique will be discussed in Chapter III.

2.5 Dynamic Properties of Rock Media

2.5.1 Seismic Velocity

The velocity of propagation of waves through rock depends on many factors which include the state of stress, magnitude of the stress wave,

water content, rock porosity, temperature and direction of propagation with respect to stratification. The compressional and shear wave velocities, C_p and C_s, are given by

$$c_p^2 = \frac{E(1-\nu)}{\rho(1+\nu)(1-2\nu)} \qquad (2.3)$$

$$c_s^2 = \frac{E}{2\rho(1+\nu)} \qquad (2.4)$$

The relation between C_p and C_s is expressed as

$$C_p = \sqrt{3}C_s \quad \text{for} \quad \nu = 0.25 \qquad (2.5)$$

For low intensity stress waves travelling through a material, there is no shear in the medium and the seismic velocity is due to a compressional wave only which can be approximated by

$$c_l^2 = \frac{E}{\rho} \qquad (2.6)$$

2.5.2 Dynamic Stresses Around a Cylindrical Cavity

The free field solution for the stresses around a cylindrical cavity due to an incident wave propagating through an elastic media has been given by Pao and Mow (24). The reference also gives the stresses around the cavity reinforced by a rigid body. The mathematical solution for the interaction problems is restricted to cavities with regular shapes.

2.5.3 Wave Propagation in One Dimension

Some of the characteristic features of wave motion in a continuum can be determined by analysis based on one-dimensional geometry. In pure one-dimensional longitudinal motion all material particles move along parallel lines, and the motion is uniform in planes normal to the direction of motion. Clearly, one length coordinate and time are sufficient to

describe one-dimensional longitudinal motion in a continuum. The differential equation for one-dimensional wave propagation is

$$\frac{\partial^2 U}{\partial x^2} - \frac{\rho}{E} \frac{\partial^2 C_p}{\partial t^2} = 0 \qquad (2.7)$$

The solution has the general form

$$U = f(C_p t + x) + h(C_p t - x) \qquad (2.8)$$

Thus, the wave travels with a compressional wave velocity C_p, and propagates without distortion, being only changed by reflection or, refraction at discontinuities in the medium.

To get the longitudinal frequency and period of vibration of an elastic bar, U is assumed in the form

$$U(x,t) = G(x) \cdot \text{Sin} (\omega t + \theta) \qquad (2.9)$$

Substituting into equation (2.7) and solving gives

$$G = C_1 \cos \frac{\omega x}{C_p} + C_2 \sin \frac{\omega x}{C_p} \qquad (2.9)$$

The general solution for vibration is given by

$$U = \sum_{n=1}^{\infty} G_n (A_n \cos \omega_n t + B_n \sin \omega_n t) \qquad (2.10)$$

The constants for each mode are determined from the initial conditions.

Przeminiecki (26) has given a numerical method for solving such a problem in which the bar is divided into two elements as shown in Fig. 2.5. Taking $U_o = 0$ to represent fixation at one end

$$[K_e] = \frac{2AE}{L} \begin{bmatrix} 2 & -1 \\ -1 & 1 \end{bmatrix} \qquad (2.11)$$

$$[M_e] = \frac{\rho AE}{12} \begin{bmatrix} 4 & 1 \\ 1 & 2 \end{bmatrix} \qquad (2.12)$$

The matrix equation of dynamic equilibrium is

$$(-\omega^2 [H]_e + [k]_e) \cdot \{x\} = 0 \qquad (2.13)$$

Substituting (2.11) and (2.12) into (2.13) gives

$$-\omega^2 \frac{\rho_{AL}}{12} \begin{bmatrix} 4 & 1 \\ 1 & 2 \end{bmatrix} + \frac{2AE}{L} \begin{bmatrix} 2 & -1 \\ -1 & 1 \end{bmatrix} \{x\} = 0 \qquad (2.14)$$

For a nonzero solution for $\{x\}$, the determinant formed by the coefficients in (2.14) must be equal to zero. Making the substitution $\mu = \frac{\omega^2 \rho_0 L^2}{E}$ gives

$$\begin{vmatrix} 2(1-2\mu^2) & -(1+\mu^2) \\ -(1+\mu^2) & (1-2\mu^2) \end{vmatrix} = 0 \qquad (2.15)$$

From Eqn. 2.15

$$7\mu^4 - 10\mu^2 + 1 = 0 \qquad (2.16)$$

Hence

$$\mu_1^2 = \frac{1}{7}(5-3\sqrt{2}) , \quad \omega_1 = 1.6114\sqrt{\frac{E}{\rho_0 L^2}}$$

$$\mu_2^2 = \frac{1}{7}(5+3\sqrt{2}) , \quad \omega_2 = 5.6293\sqrt{\frac{E}{\rho_0 L^2}}$$

Values of ω_1 and ω_2 are 2.6% and 19.5% higher than the corresponding analytical values.

2.5.4 Wave Propagation in Two-Dimensions

The two-dimensional wave equation is

$$\frac{\partial^2 U}{\partial x^2} + \frac{\partial^2 U}{\partial y^2} = c_p^2 \frac{\partial^2 U}{t^2} \qquad (2.17)$$

in which $U = f(x,y,t)$

The solution of this equation is

$$U = f(c_p t + lx + my) + h(c_p t - lx - my) \qquad (2.18)$$

The functions f and h represent plane waves propagating in the direction of a vector with direction cosines l and m.

2.5.5 Analytical Solution for Interaction Response

For any type of disturbance in a rock medium surrounding the structure, the responses of the structure and the medium are interactive. This problem, termed soil-structure interaction, is of considerable interest in modern structural dynamics.

Several types of finite elements are available to solve soil-structure interaction problems; three-dimensional solid elements, axisymmetric solid elements and two-dimensional plane strain elements. The soil-structure model can be either analysed as single unit or the system can be solved by substructuring.

Blakey (6) solved the problem by considering the soil-structure model as a single unit and taking into account damping between elements only. Boundaries were set at sufficient distance from the structure to avoid errors due to reflection at the boundaries.

The substructuring technique was applied by Atchison (2) for underwater structures. In the first stage the response of the medium and the consequent pressure on the structure were determined assuming the structure to be rigid. In the second stage external loads are applied to the structure to simulate the pressure obtained from the first stage and the response of the structure and medium are obtained. The final solution is the superposition of the two stages. This approach can be applied for studying the soil-structure interaction by using the appropriate equations for wave propagation and stiffness for the rock media.

Liaw and Chopra (18) used the substructuring technique for studying the response of axisymmetric towers partly submerged in water to earthquake ground motion. The structure and the body of water are considered two

substructures. The equations of motion for the structure are developed in terms of its modal coordinates including terms associated with hydrodynamic interaction. The finite element method is used to obtain displacements of the tower. The terms associated with hydrodynamic interaction in the modal equations of motion are determined by solving the Laplace equation governing the dynamics of incompressible fluid. This approach can be utilized in solving interaction problems in rock by considering rock-structure interaction instead of hydrodynamic interaction.

2.6 Underground Nuclear Power Plants (UNPP)

Public resistance to the siting of nuclear power plants in the vicinity of metropolitan areas in view of ecological problems has prompted the investigation of alternatives, such as underground and offshore plants with inherent advantages of biological shielding. This study will be restricted to underground plants.

2.6.1 Advantages of Underground Siting

The advantages of underground siting in some situations may more than compensate for added costs making them preferable even when surface sites are available. By virtue of greater safety, reduced surface area requirements, and improved aesthetics, underground sites can be found where acceptable surface sites are not available. Reddy and Kierans (27) state one of the advantages as

the reduction in complexity of seismic amplification by virtue of location in a continuum compared by surface structures and the support provided by the rock media to the functional structures such as a turbine generator system. Current exploratory techniques for the location of an underground site involving tunnels will expose faults which is not the case for surface siting which may involve risk of an undetected hidden fault.

UNPP offer effective containment in the event of loss of primary contain-

ment and possible shutdown.

2.6.2 Depth of Burial

For rock to provide effective radiation shielding, the depth of burial must be sufficient to prevent cracks from opening to the surface under the influence of increased cavity pressure following an unexpected accident. Also, the structure should be deep enough in rock media to avoid the effect of wave reflection at the free surface.

To estimate the required depth of burial, a study was performed by Watson, Kammer, Langely, Selzer and Beck (33) for the distribution of rock stresses between an unlined cavity and the surface for different cavity pressures. The results are reproduced in Fig. 2.6. The net tangential stress, σ_t, obtained by combining the lithostatic and internal pressure components, varies between the cavity and the surface from tension to compression. Due to the low and unpredictable tensile strength of most rock media, cracks are likely to open wherever a tensile stress exists allowing direct flow to the atmosphere (failure of the rock containment). Fig. 2.7 shows the minimum depth of burial as a function of cavity pressure for the no tensile stress condition.

2.6.3 Types of Underground Openings

Underground openings can be broadly classified as configuration types and structural types.

2.6.3.1 Configuration Types

Configuration of underground openings may vary according to the kinds of equipment to be installed, types of media or the design considerations.

Table 2.1 shows typical underground openings that have been adopted for underground power plants.

2.6.3.2 Structural Types

Fig. 2.8 indicates the basic types of underground openings as given by Kierans, Reddy and Beale (13) which are outlined below:

i) Cut-and-Cover Structure. This type is suitable for non-massive and poorly cemented materials. The roof and wall liners are designed to carry the soil overburden.

ii) Unlined Cavity. This type of cavity is usually suitable for non-faulted massive rock. Rock bolting patterns are required to provide adequate structural integrity against creep or seismic wave.

iii) Lined Cavity. The lining is usually composed of concrete or steel or both, to provide additional protection or to cope with hydro-logical conditions. Under certain conditions, linings may reduce stresses in the medium. However, the effects of very soft liners are negligible.

iv) Lined Cavity with Annular Filling. A soft annular filling, such as foamed cement, can be used to permit possible ground motions of 5 to 6 feet in shear zones adjacent to faults without damage to the internal lining. The integrity of the tunnel lining for bending in the longitudinal direction should be checked approximately by using the concept of beam on elastic foundation. To minimize the high straining actions produced in the longitudinal direction, the tunnel should be provided by joints at reasonable distances along its length.

v) Multiple Cavities. The refined dynamic analysis for multiple cavities is complicated by problems of interaction. For approximate dynamic analysis the separating media may be ignored and an enveloping

opening can be considered. The finite element technique provides solution for the static problem considering the separating media. As a structural requirement, the distance apart should not be less than twice the cavity span.

2.6.3.3 Types of Liners

Several types of liners are commonly used to i) provide support for the cavity wall, ii) prevent radiation leakage, and iii) make the underground openings serviceable. Figs. 2.9a and b indicate some types of liners suggested by Ref. 33.

i) **Steel Liners.** Liners constructed from steel plates of different thicknesses provide good protection against radiation leakage and are easy to install. The disadvantages are higher costs and temperature conductivity.

ii) **Reinforced Concrete Liners.** These are usually constructed with a non-reinforced concrete structural inner plate to provide leak protection. The costs are lower but large thicknesses are required.

iii) **Composite Steel and Concrete Liners.** These are the most suitable from the structural standpoint.

iv) **Steel Ribs and Posts.** Fig. 2.10 shows a steel rib and post liner system suggested by Parker and Semple (25). Steel posts in fractured and jointed rock formations are usually loaded out-of-plane causing torsion and biaxial bending. Steel sets fabricated from circular pipe or tubular box-shaped sections have been recommended because the closed structural shape of a box section resists nonuniform torsional and lateral loads more effectively. Filling the pipe sections with concrete results in considerable saving of steel.

v) <u>Wire Fibre Reinforced Concrete</u>. Wire fibre reinforced concrete made with high, very early strength regulated-set cement was suggested (25) as a tunnel support material. The lining can be placed by a slip form located immediately behind and contiguous with a tunnelling machine.

iv) <u>Prestressed Concrete Liners</u>. This is a current trend in lining which eliminates most of the disadvantages of reinforced concrete liner such as low tensile strength, permeability, thick cross sections, and also closure of cracks (most important).

2.6.4 Use of Prestressed Concrete as Liner

Prestressed concrete has found wide applicability in underground power plants by its inherent advantages over steel and reinforced concrete. It gives considerable freedom in the realization of any shape of the opening considered to be advantageous in the structural or functional sense. It also affords the possibility of arranging ducts or any special channels within the cavity and increases structural safety.

2.7 Rock Bolting

The use of rock bolting makes underground structures 'self supporting.' The principal function of rock bolting is to reinforce and support the vulnerable, highly stressed portion of the rock from failing under the action of gravity and other 'in-situ' stresses. Moreover, as opposed to other methods of supporting local areas of rock, rock bolting is superior in a number of ways. In some instances, underground structures, that would not be serviceable if the surface rock were not stabilized and that would become too costly if supported with linings, are made serviceable within economic limits through the use of rock bolting.

2.7.1 Passive and Active Rock Bolting

Rock bolts consist of steel cables or bars in a borehole in rock. They were first used as dowels -- passive reinforcement -- in which the reaction force of the bolts (up to a maximum of its yield load) is available to resist rock load after a slight rock movement, approximately equal to the width of the crack in the rock. They also prevent sliding between rock layers. On the other hand, these bars or cables may be pretensioned inducing compression in the adjacent rock mass and thereby improving its properties. This type of rock bolting is termed active and is different from passive primarily in its greater length, strength and loading capacity.

2.7.2 Rock Bolt Applications

i) Radial confinement of underground roofs and walls (Fig. 2.11a).

ii) Horizontal precompression of rock pillar to increase its vertical capacity (Fig. 2.11b).

iii) In open pits, rock anchors may be used to retain loose blocks in the slopes, or to create pressures on joints or faults to prevent slips (Fig. 2.11c).

2.7.3 Rock Bolt Behaviour

At least three theories have been advanced to explain rock bolt action and to guide its design as rock reinforcement.

i) In laminated rock, the bolt stresses are thought to increase interlayer shear strength (Fig. 2.12) resulting from the clamping action of tensioned rock bolts, thereby stiffening the roof into a load-carrying beam.

ii) Another approach suggests that the radial confinement offered by the average pressure supplied by the bolts raises the strength of the

rock around the gallery.

iii) Present design is generally based on previous experience and empirical criterion based on the rock behaviour. The major attention seems to be focussed on controlling the failure of the critical regions.

2.7.4 Variables Controlling the Design of Rock Bolts

A number of interrelated variables have to be considered in designing rock bolt patterns.

2.7.4.1 Bolt Length

Bolts must be long enough to extend through the wedges which are determined to be capable of displacing into the opening. Another criterion is that bolts extend through the zones where tensile stresses are perpendicular to the opening walls. In case of openings with vertical side walls, bolts should be extended horizontally through the side walls to prevent lateral buckling of the slab into the opening due to any existing planes of weakness.

For all the above criteria, the bolt length should be directly proportioned to the span of the opening, and should be greater for flat surfaces and less for curved surfaces. From practical experience, rock bolt lengths ranging between 0.2 to 0.4 span in the crown and 0.1 to 0.5 height on the side walls are recommended.

2.7.4.2 Bolt Spacing

The first criterion for selecting bolt spacing is the support pressure required to maintain stability. Also, rock quality governs the spacing between rock bolts. Higher support pressures would be required

for flatter roofs which means closer bolt spacings.

2.7.4.3 Bolt Size and Orientation

As the size of the opening increases, the support pressures required to maintain stability also increase, necessitating large size bolts for larger openings. Sometimes it is economical to combine widely spaced long, high capacity bolts with short, low capacity bolts in between. The orientation of rock bolts is not necessarily optimum when placed at right angles to joints or laminated planes. Of course a maximum normal stress is induced along sliding planes when the prestressed bolt acts normally to the plane. However, in general for bolted systems it is more beneficial to develop the tensile capacity of the bolt than to attempt to develop its shear strength. The reason for this is that when shearing occurs by movements along the joints in rock, failure of the rock will occur by crushing at the joint around the rock bolt due to the great modulus difference. Thus it is important to orient the rock bolts in opposition of the forces acting in them from the rock mass so that the tensile capacity of the rock bolt is called into play. In general, this means placing the bolt anchored upwards as much as possible, relative to the failure plane. This is a process of optimization in a rock bolt design.

CHAPTER III

FINITE ELEMENT APPLICATION

3.1 Stress Analysis Methods for Underground
     Cavities

Exact analytical investigations are restricted to simple shapes
(circular, elliptical, etc.) expressible by simple equations. Furthermore,
the medium is usually assumed to be continuous, homogeneous, isotropic and
elastic. The irregular shapes used in practice coupled with the interaction
of the adjacent cavities makes exact analytical solutions impractical.

Experimental techniques such as photoelastic and mechanical
modelling are costly, time consuming and may involve considerable problems
of simulation. The finite element approach has proven to be one of the
most powerful methods for analysis of underground cavities that can take
into consideration changes in material properties of the surrounding media,
geometry and loading on the cavity.

3.2 Geotechnical Considerations

The increasing trend towards large permanent underground structures
in rock at depths in excess of 1000 feet located in very diverse geologic
environments, demands considerable expertise in rock mechanics. In recent
years, there has been some controversy regarding the validity of applying
elastic stress analyses to rock masses. For example, Trollope (31) has
recommended that such analyses be based upon a discontinuum mechanics
approach. Zienkiewicz (35), on the other hand, contends that elastic

19

continuum analyses are valid if the results are interpreted on a macroscopic scale with careful consideration given to joint effects. In general, it is possible to assume linear load-deformation relationships and constant elastic parameters as long as rock masses exhibit linear behaviour over the range of stress levels encountered with no slippage along joints. The in-situ deformation modulus has almost always been less than the modulus obtained from intact core specimens mainly due to the effect of joints. The ratio of these values has been observed to vary between wide limits (generally 2 to 10) and is a function of the physical characteristics of the joints and other internal flaws and fractures. Thus, the evaluation of deflections must be based on the deformation modulus derived from field measurements. In a homogeneous, isotropic medium, stresses are independent of the elastic modulus. Thus, for preliminary analysis of rock masses which approximate this condition, reliable stress predictions can be made without an accurate elastic modulus. Obviously, in-situ stresses at any point are related to the weight of the overlying rock, but there are other factors that influence the stresses such as tectonic activity and inelastic behaviour during erosion. It was shown, for example, that the horizontal compressive stresses are often much larger than the vertical stresses.

3.3 Simulation of Boundary Conditions

The true simulation of boundary conditions presents some difficulties in the modelling of the infinite medium as a finite region. The problem of wave reflection at a fixed boundary implies simulating the infinite boundary in case of dynamic analysis different than static.

3.3.1 Static Loading

Two methods for simulating the boundary conditions in this case

have been discussed by Benson, Kierans and Sigvaldson (4) and will be discussed herein. In the first approach, the bottom boundary is restrained vertically allowing only for horizontal movements. To prevent rigid body motion, only one node was restrained from both horizontal and vertical displacement (Fig. 3.1). In-situ stresses are applied along the vertical and upper sides of the relaxed rock mass, with the deadweight of the rock being assigned to the nodes in accordance with defined principles that will be explained later. It can be seen, however, that the nonuniform side loading may be represented by a combination of axial forces and bending moments. In the absence of cavities, such a loading produces identical stress conditions on every vertical section accompanied by a bending effect resulting from the bending moment. This causes an upward arching of the rock mass at the top which is partially restrained at the bottom due to the condition of zero displacement.

In the second approach, all the boundaries are fully restrained against perpendicular movements as shown in Fig. 3.2. The rock mass is assigned its assumed initial in-situ stress state with the deadweight of the rock mass assigned to the nodes as before. The resulting equivalent nodal forces vanish at all interior nodes except at the internal boundaries where force resultants act into the opening. It must be pointed out that, as the two cases considered a vertical axis of symmetry, only one-half of the model needs to be analysed imposing horizontal restraints at the axis of symmetry.

3.3.2 Dynamic Loading

Lysmer and Kuhlemeyer (19) formulated a general method in which an infinite system is replaced by a finite system with absorbing boundaries.

The dynamic response of the interior region is determined from a finite model consisting of the interior region subjected to boundary conditions, which ensures that all energy arriving at the boundaries is absorbed (Fig. 3.3). On the other hand, Moselhi (20) used displaced boundaries to simulate an infinite medium. At each node on the boundaries vertical and horizontal springs were introduced to represent vertical and horizontal resistance of the rock. Damping is allowed between the finite elements within the region. The proper evaluation of the spring stiffness should include the elastic and dynamic properties of the rock media. Blakey (6) used a simple approach to avoid deflection of the waves at the boundaries by restricting the analysis to be confined to the time period required for the wave to reach the nearest boundary. This is a valid assumption for blast loading (short duration) but not so for seismic loading (long duration).

In this thesis, the boundaries are located a sufficiently large distance from the structure to ensure that the results at the interface are not affected by reflection at the boundary. Energy absorbing boundary conditions are not considered.

3.4 Dynamic Analysis of Finite Element Method

$$[M]\{\ddot{X}\} + [C]\{\dot{X}\} + [K]\{X\} = \{P\} \quad (3.1)$$

3.4.1 Mass Matrix [M]

The simplest mathematical model is the lumped mass representation in which the concentrated masses are placed at the node points at the locations of the postulated element degrees of freedom. The masses are calculated by assuming that the material within the mean locations on either side of the specified displacement for each element behaves like a

rigid body while the remainder of the element does not participate in the motion. This assumption, therefore, excludes dynamic coupling between the element displacements, and the resulting element mass matrix is purely diagonal. It has been demonstrated that for a given number of degrees of freedom the lumped mass representation is less accurate than the equivalent mass matrices derived on the basis of inertia forces acting on the assembled structure. However, in many practical applications it is preferable to use the lumped-mass matrices because of the significant computational advantages in the use of diagonal matrices.

3.4.2 Damping Matrix [C]

The numerical value of the damping coefficient can be expressed in the form

$$C = C_1 M + C_2 K \qquad (3.2)$$

where C_1 and C_2 are constants.

This assumes that damping is not a single constant for all modes but is proportional to density and stiffness. Most media, such as rock, have damping values (C) far below the critical damping value (C_c).

Now

$$C_c = 2\sqrt{KM} = 2M\omega \qquad (3.3)$$

$$\int (\text{damping ratio}) = \frac{C}{C_c}$$

For the n-th mode of any system for which damping is expressed by Eqn. 3.2

$$\int_n = \frac{C_1 M}{2\sqrt{KM}} + \frac{C_2 K}{2\sqrt{KM}} \qquad (3.4)$$

or

$$\int_n = \frac{C_1}{2\omega_n} + \frac{C_2 \omega_n}{2}$$

The minimum damping ratio ζ_n and the corresponding natural frequency ω_n can be obtained by differentiating ζ_n with respect to ω_n and setting the resultant derivative equal to zero which gives

$$\omega_n = \sqrt{\frac{C_1}{C_2}} \qquad (3.5)$$

Assuming equal contributions from the additive terms of equation (3.5) the constants C_1 and C_2 may be calculated as

$$C_1 = \zeta_n \, \omega_n \qquad (3.6)$$

$$C_2 = \zeta_n / \omega_n \qquad (3.7)$$

or in terms of the period of the system

$$C_1 = 2\pi \zeta_n / T_n \qquad (3.8)$$

$$C_2 = \zeta_n T_n / 2\pi \qquad (3.9)$$

In practice one of the two constants C_1 or C_2 is specified and the other sets equal to zero.

3.5 Finite Element Applications to Reinforced and Prestressed Concrete

Non-homogeneous nature presents no difficulty as elements can have different material properties and shapes; e.g. two-dimensional elements can represent concrete and rock media while line elements can represent steel reinforcements or liners.

3.5.1 Special Considerations for the Mathematical Model

The difficulties in studying the behaviour of reinforced and prestressed concrete members arise from the following facts:

i) Representation of bond between steel and concrete.

    ii) Non-linear behaviour of the concrete material.

    iii) Influence of shrinkage and creep on concrete deformation.

    iv) Small tensile strength values causing cracking at normal

        working loads.

In the following, the factors will be discussed separately.

3.5.1.1 Bond Between Steel and Concrete

Bond representation between steel and concrete elements and bond slip is difficult to incorporate in the analysis. The two methods used are:

    i) Introduction of a "boundary layer" of special elements concentric with the bar immediately adjacent to it and of different characteristics. This method has yet to be used in view of the complexity of the analysis.

    ii) The second method is to use closely spaced discrete spring linkages of zero length to connect steel and concrete elements as shown in Fig. 3.4. The figure shows the approximation of the rounded steel bars to square ones of side length $\frac{MD\sqrt{\pi}}{2}$ where M is the total number of bars and D is the bar diameter. This allows the use of a reduced cross section width at the level of the steel reinforcement. The stiffness values for the springs can be obtained experimentally from the relation between bond stress and bond slip. The nodal displacements for the structural members are obtained from which the bond stresses and consequently bond slip can be obtained. The bond linkage element is assumed to fail, and consequently the connected steel element, if bond slip reaches a peak value determined experimentally. In this study, full bond between concrete and steel elements is assumed in the range of loads applied.

3.5.1.2 Non-linear Behaviour of Concrete
Material

The stress-strain relationship for concrete is non-linear and a function of many variables while that of steel is linear up to yield.

In the "variable stiffness matrix" approach the elasticity matrix is written as

$$[D] = [D \cdot (\{\varepsilon\})]   \qquad (3.10)$$

As the elasticity matrix [D] influences the final stiffness matrix, the equilibrium equations become

$$[K \cdot (\{\delta\})] \{\delta\} = \{P\} \qquad (3.11)$$

So, at every level of the stress state reached, the strains can be obtained and a new elasticity matrix formulated to determine the final stiffness matrix. New values of displacements, stresses and strains can be obtained after applying another increment of load (Fig. 3.5). This method is very time consuming.

In the "initial strain method" the constitutive relations are of the form

$$\{\varepsilon\} = f(\{\sigma\}) \qquad (3.12)$$

For every increment of load the elastic strains can be obtained and the stresses calculated using the initial elasticity matrix. The inelastic strains can be obtained using Eqn. 3.12 and the difference between the elastic and inelastic strains can be related to the nodal forces. These new forces are applied to the structure and new values of stresses and strains obtained. These values are added to the initial values and the iteration continued until the nodal forces produced from the initial strains become very small, then another increment of load is applied. This method fails to converge for perfectly plastic or for work hardening

materials of very small degree.

In the "initial stress" method the elastic strains are obtained by applying an increment of load. The elastic stresses are determined using the elasticity matrix. The relation

$$\{\sigma\} = g\,(\{\varepsilon\})\qquad(3.13)$$

can be used to obtain the plastic stresses and the differences between these and the elastic values give the initial stresses that can be transformed to nodal forces. These forces can be treated in the same manner as in the initial strain method and when they become small a further increment of load is applied until failure. Schematic sketches for the three methods explained are indicated in Figs. 3.5a and b.

3.5.1.3 Limiting Tension of Concrete

In some approaches cracking has been represented by separating the concrete elements at their common edges and assigning a different nodal point number on each side of the crack (Figs. 3.6a and b). In other approaches the cracks are represented by separating the element into two parts keeping the numbering system unchanged (Fig. 3.6c) and introducing a zero elasticity constant (E) for the cracked element. The direction of the crack is taken perpendicular to the direction of the tensile stress. In the case of prestressed concrete this problem does not arise as all the members are mainly in compression.

3.5.2 Transfer Prestress from Steel to Concrete

Prestressing forces are transmitted from the steel elements to the concrete elements through bond that is assumed to be completely developed between the two types of elements. The steel elements are assumed to have

prestress equal to the initial stress in the bar. This can be changed to prestrain simply by dividing by the elastic modulus E. The strains are then converted to equivalent nodal forces in the direction of local axe (Fig. 3.7a) as given by the equation

$$\{F_{oe}\}_{4 \times 1} = EA\varepsilon_o \left\{ \begin{array}{c} -1 \\ 0 \\ 1 \\ 0 \end{array} \right\}_{4 \times 1} \tag{3.14}$$

The transformation matrix for one node (Fig. 3.7b) [r] is

$$[r]_{2 \times 2} = \begin{bmatrix} \text{Cos} & -\text{Sin} \\ \text{Sin} & \text{Cos} \end{bmatrix} = \begin{bmatrix} C & -S \\ S & C \end{bmatrix} \tag{3.15}$$

For a member of two nodes the transformation matrix [R] is

$$[R]_{4 \times 4} = \begin{bmatrix} r & 0 \\ 0 & r \end{bmatrix} = \begin{bmatrix} C & -S & 0 & 0 \\ S & C & 0 & 0 \\ 0 & 0 & C & -S \\ 0 & 0 & S & C \end{bmatrix} \tag{3.16}$$

The initial nodal force matrix in global coordinates $\{F_o\}$ is given by the equation

$$F_o{}_{4 \times 1} = [R]_{4 \times 4} \{F_{oe}\}_{4 \times 1} \tag{3.17}$$

$$\{F_o\}_{4 \times 1} = EA\varepsilon_o \left\{ \begin{array}{c} -C \\ -S \\ C \\ S \end{array} \right\} \tag{3.17}$$

These forces are added properly to the matrix of external forces acting on the structure. The final stresses in the steel elements are those due to the external forces plus those due to the initial prestress (with the proper sign conventions). Appendix A gives the formulation of the bar element stiffness matrix in the global system.

3.6 Thermal Stresses

Following loss of coolant accidents, in power plants for instance, the temperature within the containment could rise. This will result in stress gradients across the containment walls. Watson (33) calculated the resulting stress distributions in liner walls using analytical solutions assuming that the liner is prevented from lateral expansion by the surrounding rock. This is a conservative approach as the in-situ rock, while admittedly stiff, is compressible. Extension of the wall liner by compressing the surrounding rock would relieve some of the stress.

The following section discusses the analysis of the problem by the finite element method. The compressibility of the rock media is permitted by not changing the elastic properties of the rock.

3.6.1 Nodal Forces Due to Initial Strains

Thermal stress analysis by FEM is similar to that discussed before for the prestressing forces. The difference lies only in the fact that thermal strains are present in two-dimensional elements while the prestrain acts only along line elements. The method will be applied to triangular plane stress elements. The same procedure can be followed for rectangular elements in the computer programme. A temperature rise within the element of $\triangle T$ will result in the initial strain matrix

$$\left\{ \varepsilon_o \right\}_{3 \times 1} = \alpha \cdot \triangle T \cdot \begin{Bmatrix} 1 \\ 1 \\ 0 \end{Bmatrix} \qquad (3.18)$$

in which α is the coefficient of thermal expansion. These initial strains are converted to initial nodal forces $\left\{ F \right\}_o^e$ using the following energy equation:

$$\{F\}^e_{\xi_o} = - \int [B]^T_{6\times3} \ [D]_{3\times3} \ \{\xi_o\}_{3\times1} \ d \ (vol) \quad (3.19)$$

$$= - [B]^T \ [D] \ \{\xi_o\} \int d \ (vol)$$

$$\{F\}^e_{\xi_o} = - [B]^T \ [D] \ \{\xi_o\} \ At \qquad (3.20)$$

in which

     A   is the area of triangular element

     t   is the constant thickness of the element

     $[B]^T$ the transpose of the strain matrix

     $[D]$ the elasticity matrix of the material

$$[B]^T_{6\times3} = \begin{bmatrix} -Y32 & 0 & -X32 \\ 0 & -X32 & Y32 \\ -Y31 & 0 & X31 \\ 0 & X31 & -Y21 \\ Y21 & 0 & -X21 \\ 0 & -X21 & Y21 \end{bmatrix} \qquad (3.21)$$

in which X21, X31 .... are the differences in nodal coordinates X and Y in

the directions defined by the sequence of the subscripts, 1, 2 and 3 as

shown in Fig. 3.8. The elasticity matrix is

$$[D]_{3\times3} = \frac{E}{1-\nu^2} \begin{bmatrix} 1 & \nu & 0 \\ \nu & 1 & 0 \\ 0 & 0 & \left(\frac{1-\nu}{2}\right) \end{bmatrix} \qquad (3.22)$$

The computer programme performs the matrix multiplication in equation 3.20.

     The resulting initial nodal forces will be added properly to the

matrix of external forces that are assumed to be acting on the structure.

The final stresses and strains in the triangular elements are those due to

the applied forces plus the initial values with the proper signs.

3.7 Initial Stresses

As stated in item 3.3.1 the rock elements will be assigned initial stress values equal to the in-situ stresses at the particular location for studying the induced stresses due to an excavation. The solution is obtained by a procedure similar to that in thermal stress calculation in section 3.6.1. The initial stresses are transformed into initial strains by the equation

$$\left\{ \varepsilon_o \right\}_{3 \times 1} = [D]^{-1}_{3 \times 3} \left\{ \sigma_o \right\}_{3 \times 1} \qquad (3.23)$$

Using Eqn. 3.20, the initial strains are transformed to initial nodal forces added properly to the force matrix for displacement calculations. The final stresses and strains in the elements are those due to the applied forces plus the initial values with the proper signs.

3.8 Finite Element Modelling

Because the finite element model is an approximate representation, considerable care must be exercised in the establishment of the analytical model to ensure that significant errors are not introduced into the results because of inadequate modelling. In the following a brief discussion will be made for the several factors to be taken into consideration in establishing the analytical model.

3.8.1 Element Type and Mesh Size

Kulhawy (17) showed that linear strain quadrilateral elements are the most appropriate for use. Higher order elements provide additional degrees of freedom which are unnecessary in most geotechnical applications. The boundaries of the finite element mesh should be located at least 6 radii away from the centre of the opening to ensure that the computed

stresses and displacements are within an error of less than 10% of the theoretical. It was also shown that within these boundaries 125-150 elements suffice for analyses of simple structures in homogeneous rock where there is a plane of symmetry and only one-half of the system need be analysed. Regarding the element length, Kuhlemeyer and Lysmer (16) recommended a maximum element length equal to one-eighth of the wave length of the slowest body wave propagating in the elastic material for the analysis of two- or three-dimensional layered media.

3.8.2 Finite Time Increment

Higher frequency response is very important for wave propagation problems particularly for discontinuities in velocities and accelerations. If the response in the region around the discontinuity is of interest, a very small time step should be used. The characteristics of Eqn. 3.1 are best defined in terms of its natural frequency and mode shapes. For a discretized system a maximum limit of these frequencies is called the cutoff frequency or the stiffest system component. If this discretized system is excited by forcing functions having a frequency content above the cutoff frequency, such as those induced in a wave propagation problem, noise is generated in the cutoff modal response. Nickell (22) indicated that if the time step of integration is reduced in order to accurately integrate the stiff components, then the step will be too small for the lower frequency responses, resulting in excessive computer time for the calculations. On the other hand, if the time step is chosen with regard for the low-frequency response, instability will result for explicit methods and integration errors will give inaccurate solutions for the stiff

components. Table 3.1, reproduced from Ref. 6, outlines the recommenda-
tions of different authors which indicate a range of $\frac{1}{40} < \frac{\triangle t}{T_{min}} < \frac{1}{4}$.

CHAPTER IV

THE COMPUTER PROGRAMME

4.1 Introduction

Yu and Coates (34) presented a computer programme to determine the static stress distribution around typical, irregularly shaped mining openings. The programme takes into consideration non-homogeneous mechanical properties of the rock and the stresses produced by either or both gravity and tectonic forces. The computer programme in Ref. 6 is a simple plane stress analysis for dynamic behaviour of circular openings in rock. Different types of elements such as triangular, rectangular, bar and curved elements with bending stiffness are constructed.

4.2 Comparative Study

The four computer programmes considered were 1) STRUDL-II, ii) SAP-IV, iii) Yu and Coates programme (34), and iv) Blakey's programme (6). The only difficulty encountered in STRUDL-II and SAP-IV was the absence of curved elements with bending stiffness. The work of Ref. 34 was restricted to static analysis. Hence, Blakey's programme seemed to be the most suitable.

As the problems studied were beyond the scope of Blakey's programme, extensive modifications had to be made. In the following, a general description for this programme will be presented followed by an explanation of the modifications and extensions to accommodate different kinds of loading and geometry.

34

4.3 The Blakey Programme (6)

The principal part is the MAIN routine from which all other
subroutines are called. A flow-chart is given in Fig. 4.1 for the main
procedures followed within the programme.

In MAIN, all the input data for the problem are read and checked
for any input error. There are several subroutines for stiffness and
stress calculations in the programme. These are ASSEMB, BAR, TRIAN, RECT,
SHELL, ARC, LOAD, RECURS, SHELLS, RECTS, TRIST and MATINV. In the following
a brief description for each subroutine will be performed.

4.3.1 Subroutine ASSEMB

Subroutines BAR, TRIAN and RECT are called from this subroutine
after making the proper check for the calculation of the stiffness matrices
for bar, triangular and rectangular elements respectively. After that, it
calculates the mass matrix in the form of lumped masses at the proper node
and assembles the element stiffness matrices into a banded global stiffness
matrix. The proper boundary conditions are inserted and the cutoff
frequency ω_{max} and the corresponding period of vibration T_{min} calculated
in a very rough manner. The first increment of load matrix is prepared by
calling subroutine LOAD. Subroutines BAR, TRIAN and RECT are utilised for
element stiffness calculations as previously indicated.

4.3.2 Subroutine SHELL

Subroutine ARC is called from this subroutine for the formation of
the stiffness matrix of each segment of the circular liner. The elemental
stiffness matrices are superposed in an appropriate manner to form the
shell stiffness matrix. The contribution from the liner elements to the
mass matrix is also computed in this subroutine. The overall shell stiff-

ness matrix is assembled on the basis of three degrees of freedom at each node, viz. horizontal and vertical displacements and rotation. Rearrangement of this matrix is made to move rotational terms to the bottom of the matrix to take advantage from the fact that the corresponding moments in the matrix of external loads are zeroes. At the end of the subroutine, the overall shell stiffness matrix representing the circular liner is transformed to the overall banded stiffness matrix of the structure.

4.3.3 Subroutine ARC

This subroutine forms the element stiffness matrix for any segment of the circular liner (arc) in local coordinates and transforms it to the system coordinates. Under certain conditions, this subroutine rearranges the element stiffness matrix of the arch to shift rotational terms to the bottom.

4.3.4 Subroutine LOAD

The programme calculates the increment of the load to be used in the matrix of external forces for a corresponding increment of time according to the load-time function provided within the data in the MAIN routine.

4.3.5 Subroutine RECURS

The equations of dynamic equilibrium are solved to give the displacements. The resulting displacements, always functions of time, are put into the matrix of external forces to reduce core storage size.

4.3.6 Subroutine SHELLS

This determines the forces and bending moments for the curved elements and prints the resulting values for each element.

4.3.7 Subroutine RECTS

Within this subroutine, stresses for the bar and rectangular elements are calculated after making the proper checks. The principal stresses and the angles of inclination for the rectangular and triangular elements are calculated at the end of the subroutine. Stresses, principal stresses and the angles of inclination are then printed.

4.3.8 Subroutine TRIST

It is called from RECTS, after the proper check, for stress calculations. Principal stresses are calculated and printed in subroutine RECTS.

4.3.9 Subroutine MATINV

The name implies the operation of MATRIX INVERSION.

4.4 Comments on Blakey's Programme

This programme was limited to the dynamic analysis of circular openings in rock media. Although the analysis is indicated for plane strain problems, the programme solves plane stress problems only. Again, there was some restriction in feeding the data.

4.5 Modification to Blakey's Programme

In the following parts, all modifications that have been introduced to Blakey's programme will be discussed. Fig. 4.2 shows the flow-chart for the modified programme.

4.5.1 The Shape of the Opening

To make the programme applicable to all kinds of openings, the frame element was introduced to represent the liner. The procedures

followed in formulating the stiffness matrix and calculating the straining
actions for the frame elements were mainly the same as those for the curved
elements. So, the modification was done making full use of the subroutines
SHELL, ARC and SHELLS for the same purpose as outlined before. Subroutine
FRAME was only introduced to calculate the stiffnesses of the frame
elements in local coordinate system. This implies that whenever the
computation involving all subroutines, viz. SHELL, ARC and SHELLS a
variable must be used to identify the curved or frame elements. This was
done through a variable FREX (FRAME EXISTING). This variable is given a
value of 1.0 or 0.0 for frame or shell calculations respectively. At the
final stage, the straining actions for the frame elements were printed
following those for the curved elements in the same form.

The stiffness matrix for the frame element is given in Appendix A.

4.5.2 Prestressing

In order to study prestressed concrete liners and rock bolting as
active reinforcement, bar elements were used. At the same time bar
elements without prestress are treated as normal steel reinforcement.

The programme was modified to allow for initial stresses to be
given to the bar elements to represent prestressing for both cases. This
was introduced in subroutine BAR as an auxiliary part. The analysis for
this is given in Chapter III, item 3.5.2.

4.5.3 Thermal Stresses

A part of the analysis was devoted to the study of the effect of a
temperature rise in the tunnel following an accident which causes strains
in the liner and the surrounding media affecting the stress distribution
in both. To take this effect into consideration, initial strains were

given to the triangular elements and initial and final stresses are obtained. This was done partly in ASSEMB and partly in TRIAN. The analysis is given in Chapter III, item 3.6.1.

4.5.4 In-situ Stresses

As stated before, any excavation in rock is preceded by an in-situ stress state due to geological considerations. The complete analysis of the problem should take these stresses into consideration. Initial stresses were given to the triangular elements to account for the in-situ stresses from which initial strains are calculated and the procedures follow the initial strain case. This was done partly in ASSEMB and partly in TRIAN. The values of the initial stresses are input as properties of the triangular elements in the MAIN routine. These values are obtained from theories that best predict the in-situ state of stress.

4.5.5 Static Analysis

The states of in-situ stress, induced stress, prestressing and rock bolting are static effects in nature. Subroutine SYMSOL was introduced to solve the equations of static equilibrium. Static nodal displacements are obtained from which stresses are calculated in the same way as in the dynamic analysis. This modification made the programme so general that it can cope with any combination of loading.

4.5.6 Body Forces

In some cases, it is required that the own weight of the elements be taken into consideration. This was accomplished by multiplying the lumped mass matrix, MASS by the gravitational acceleration and adding in the proper locations to the static load matrix XP. Variable, KHALID was

given values 1.0 or 0.0 to show whether the own weight had to be taken into consideration or not.

4.5.7 Other Considerations

As a special case, the programme solves problems of circular openings. The variable CIR was given values 1.0 or 0.0 for circular or non-circular opening. A condition was specified for plane stress or plane strain analysis by assigning the variable ABIR two values 0.0 or 1.0, for the two cases respectively. Another variable, AMAL specified the problem as static, dynamic or static and dynamic with three values, -1.0, 0.0 or +1.0 respectively.

4.6 Programme Check

First, three problems given by Blakey (6) with different load-time functions were checked after the modifications and the same results were obtained.

The beam shown in Fig. 4.3a was tested for different cases of loading. Taking advantage of symmetry, the mesh is restricted to one-fourth of the region as shown in Fig. 4.3b. The following problems were solved:

Problem No. 1. Beam axially loaded with 180 kips at node 21.

Theoretical solution

$$\sigma = \frac{F}{A} = \frac{-180,000}{20 \times 1} = -9000 \text{ psi}$$

δ (maximum horizontal displacement)

$$= \frac{FL}{AE} = \frac{180,000 \times 60}{20 \times 3 \times 10^6} = 0.18 \text{ in}$$

Finite element solution

σ ranges between -8990 and -9003

δ = 0.17 to 0.21 in

The difference is due to the fact that the F.E. solution is two-dimensional with a stress concentration at node 21.

Problem No. 2. Six prestressed steel elements at the upper boundary.

Prestress = 150 ksi

Area of steel = 1.2 in^2

Theoretical solution

Prestressing force = 150 x 1.2 = 180 kips

Equivalent area of cross section = A + $\frac{E \text{ steel}}{E}$ A$_{steel}$

$$= (20 \times 1) + \frac{30 \times 10^6}{3 \times 10^6} \times 1.2 = 32 \text{ cm}^2$$

σ_{steel} = -150,000 + 10 x 5,625 = -93750 psi

Finite element solution

σ ranges between -5580 and -5630 psi

σ_{steel} ranges between -93710 and -93210 psi

Problem No. 3. Two values of prestrain were given to the triangular elements, that is $\dot{\epsilon}_x = \epsilon_y = \epsilon = -0.003$. The member is unreinforced through the whole length.

Theoretical solution -- As there are no restraints on the member, it will contract freely without causing any stresses.

σ = 0

δ = ϵ 1 = -0.003 x 60 = 0.018 in

Finite element solution

$$\sigma \simeq -0.01 \text{ psi (negligible)}$$

$$\delta = 0.0195 \text{ in}$$

Problem No. 4. A dynamic and static analysis was carried out simultaneously in one run for an opening with vertical side walls and arched roof. In the dynamic analysis part, a load-time function as shown in Fig. 4.4 was used. The time step was 0.00005 second with total number of time steps of 120. The nodal forces produced from the dynamic load was applied as static load in the static analysis part. The results of the dynamic analysis were slightly different from those of Ref. 6 for the circular opening. Also, the ratio between the dynamic and static stresses (dynamic load factor) varied from 1.15 to 1.25.

RESULTS AND CONCLUSIONS

5.1 A Logical Insight to the Problem

Assume a certain location in rock with its in-situ state of horizontal and vertical stresses being known. After excavation of an underground opening of a certain shape, the overlying rock will tend to push the roof of the excavation downward while the surrounding rock will push the side walls inward. Depending on the depth and the ratio of horizontal to vertical in-situ stresses, the opening will take a deformed shape. A stress relief will follow this process due to the freedom given to the rock mass in this zone.

5.2 Finite Element Idealization

A constant stress-plane strain triangular element was used in this study. The boundaries of the studied region were located five radii from the centre line of the cavity so as to approximately simulate an infinite region. The rock medium and the liner were assumed linearly elastic, isotropic and of limiting tensile strength and cracks were not allowed in the range of the operating loads. These are valid assumptions in the range of loads encountered.

The in-situ state of stress was represented as an initial stress state in the rock elements. The deadweight of the rock elements was taken into consideration by assigning nodal forces to the surrounding nodes, e.g. for the constant strain triangle used, one-third of the element weight

43

is assigned to each node -- Zienkiewicz (36).

5.3 Case Studies

A full scale plane finite element model was chosen for a cavity 84 feet wide and 105 feet high. The thickness of the model was one inch as the computer programme operates on unit thicknesses of the dimensions used. The cavity was considered long enough to validate the approximation of plane strain analysis. The dimension of the studied region was 420 x 420 feet and the shape of the opening was an arched roof with vertical side walls. The properties of the rock and the depth of burial could be changed easily. Fig. 5.1 shows the general layout for applications in the mining and energy industries. The dimensions are smaller for applications in transportation.

Both static and dynamic loading cases were considered. The static loading was the in-situ stress as initially applied to the rock mass with the deadweight of each element assigned to the surrounding nodes as previously explained. The dynamic loading was a constant step pulse shown in Fig. 5.2 representing a blast excitation applied horizontally. A unit value of σ_p (normal component of stress behind and in the direction of the incident wave) was used in the computational work.

For dynamic loading, the boundaries on the right side were assumed free while all the other three sides were considered fixed. Since the stress waves reflect from these boundaries modifying the true cavity stresses, only the time history free from these effects was examined. The compressional wave velocity within the rock medium was approximately 100 inches per msec; thus, reflection from the nearest boundary will reach the cavity after about 80 msec. The duration of loading was restricted to

only 60 msec.

The model in Fig. 5.1 was analysed in three stages. First, the rock mass was subjected to an assumed value of initial compression in the vertical and horizontal directions along with the deadweight of the rock within the region. Solution of this case will give the actual state of in-situ stress within the rock media. In the second stage, an opening was introduced in the region as shown in Fig. 5.1 and the induced stresses and displacements are obtained for the unlined cavity. In the third stage, different types of liners were considered and the effects on the stresses and displacements were obtained.

5.3.1 In-situ Stresses

The uniform mesh used in solving this problem is shown in Fig. 5.3. The properties of the rock media used were as follows:

$$E = 1.5 \times 10^6 \text{ psi}$$
$$\nu = 0.3$$
$$\rho = 0.00021 \text{ lb/in}^3$$

The rock mass was given an average of precompression of 250 psi in the two directions. Under the effect of the rock weight, the vertical stress at the top reached a compression of 66 psi and the stress at the bottom 434 psi compression, both approximately equal to γh at the corresponding levels. The change in the horizontal stress was only due to Poisson's effect and the horizontal stresses varied from 329 psi from bottom to 171 psi at top. The results indicate an average ratio of 0.80 between horizontal and vertical stresses.

5.3.2 Induced Stresses

i) **Static Loading.** The finite element model used is shown in

Fig. 5.4a. The maximum horizontal displacement for the side walls was 0.123 inch inward, while the maximum vertical displacement of the arched roof (at the crown) was 0.194 inch downward. The final deflected shape of the opening after excavation is shown in Fig. 5.4b.

The whole region which was under compression before excavation experienced a relief of stress. The magnitudes varied depending upon the location. The stress relief values changed from 5% at the center of the vertical sides to 19% at the middle point of the bottom. The vertical side walls of the cavity indicated horizontal tensile stress values with a maximum of 68 psi correspond to 259 psi compression before excavation. A vertical tensile stress of 5.3 psi was obtained in the horizontal part. It is clear that for larger depths of burial or where the horizontal in-situ stresses are high, the induced tensions will be higher causing cracks in the rock before lining.

The maximum relief of vertical stresses was notified at the crown and was of the order of 60%.

ii) Dynamic Loading. Stresses within the rock media were mainly compressive with a maximum value of 1.94 σ_p. The maximum tensile stress in the vertical side walls was 0.30 σ_p.

Three locations, as shown in Fig. 5.3 -- elements 1,2 and 3 -- were chosen for studying the change of stress with time. The values were compared later with those for a lined cavity.

Figs. 5.5a, b and c show the variation of horizontal stresses up to 0.06 sec. The stresses first increase with time and then become asymptotic to the static solution. Stress reversal from compression to tension was observed at location 2. The stresses obtained by assuming the dynamic load to be a static one are also plotted. The ratio between the dynamic and static values varies with the location (range: 1.15 to 1.25).

5.3.3 Lined Cavity

Reinforced and prestressed concrete liners (R.C. & P.C.), passive and active rock bolting and steel liners were analysed for static and dynamic loading.

5.3.3.1 Reinforced Concrete Liner

This type of liner is usually used for rock of poor quality similar to that considered in this study. The concrete section is 10.5 feet thick reinforced with steel bars (1.5% of the cross sectional area) located on the interior face. The properties are as follows:

$$E_{conc} = 3 \times 10^6 \text{ psi}$$

$$\nu_{conc} = 0.17$$

$$\rho = 0.00021 \text{ lb/in}^3$$

$$E_{steel} = 30 \times 10^6 \text{ psi}$$

The steel reinforcement is represented by bar elements at the interior face neglecting the thickness of concrete cover for simplicity as shown in Fig. 5.6.

i) _Static Loading_. The maximum inward horizontal displacement of the vertical side walls was 0.101 inch and the maximum vertical settlement of the arched roof was 0.175 inch. This shows decrease of 18% and 10% in the displacements compared to the case of no lining which will be considered the reference case. The maximum vertical stress was observed at the foot of the vertical concrete wall with a value of 499 psi and the maximum horizontal stress was 420 psi. Both values are far below the concrete compressive strength of 4000 psi. Small horizontal tensile stress was produced in the vertical side walls with a maximum value of 60 psi which

is still far below the permissible concrete tensile strength of 400 psi.
The steel elements were completely in compression with a maximum value of
4797 psi while the minimum compressive strength of the steel is about 27,000
psi. The final deflected shape is shown in Fig. 5.7.

ii) _Dynamic Loading_. The maximum compressive stress in the liner
was $1.49\sigma_p^-$ at the bottom horizontal part and the maximum tensile stress
was $0.119\sigma_p$ in the vertical side walls. The stresses in the steel rein-
forcement were compressive with a maximum value of $26\sigma_p^-$.

Stresses within the rock media were mainly compressive with a
maximum value of $1.336\sigma_p^-$ -- smaller than the maximum compression in the
R.C. liner. Elements A, B and C as shown in Fig. 5.6 were studied
separately. The horizontal stress vs. time relationship for the three
elements are shown in Figs. 5.8a, b and c. Plotted on the same figures
are values of static stresses obtained by treating the dynamic load as a
static one. The dynamic stresses are generally larger than the corres-
ponding static values but smaller than those for the unlined cavity. The
stresses within the elements behaved in the same manner as previously
explained in the case of the unlined cavity.

Two steel elements D and E were chosen for the same study and the
curves of stress vs time are shown in Figs. 5.9a and b. For these
elements, the ratio between dynamic and static stresses is very high but
with no stress reversal.

5.3.2 Prestressed Concrete Liner

The two cases considered in this study are shown in Figs. 5.10a
and b. In Case 1, the prestressed steel is located on the interior face
of the cavity. In Case 2, the prestressed steel is located on the interior

face of the vertical side walls only with the ends of the cables jacked to the concrete from the exterior side at top and bottom of the walls. For both cases, the concrete thickness was 10.5 feet while the prestressed steel was 0.5% of the concrete cross sectional area. The steel bars were prestressed to 150 ksi.

i) _Static Loading_. For Case 1, the maximum horizontal displacement of the vertical side walls was 0.124 inch and the vertical settlement of the arch at the crown was 0.239 inch. The corresponding values for Case 2 were 0.09 and 0.222 inch. The vertical settlements for both cases are higher than those for the unlined case due to the effect of the prestressing at the upper ends of the tendons. The horizontal displacement in Case 2 was 28% smaller than for Case 1 and the unlined cavity. The final deflected shapes for both cases are shown in Fig. 5.7.

As a result of the prestressing effect, the vertical compressive stresses in concrete at the bottom of the vertical side walls were increased up to a maximum of 879 psi for Case 1 and 677 psi for Case 2. The corresponding value for the case of the unlined cavity was 477 psi (compression). The maximum horizontal stresses were 443 and 517 psi. There still some tensile stress in Case 1 with maximum of 54 psi while they were eliminated completely in Case 2 except in one element where the value was 53 psi. Stresses in the steel elements averaged 143 to 145 ksi indicating about 4.7% and 3.3% loss due to elastic shortening. In general, results obtained from Case 2 were better than those for Case 1. For the best redistribution of stresses in the concrete liner, more attention should be devoted to tendon profile and area of steel with reasonable prestressing force.

ii) _Dynamic Loading_. The dynamic analysis for only Case 1 will be discussed herein. However, the difference between Case 1 and Case 2 is

mainly due to the change of cable profile as the area of steel is the same.

The maximum compressive stress in the liner was $2.52\,\sigma_p$ and occurs at the same location as in the case of the R.C. liner. The maximum tensile stresses are of the order of $0.164\,\sigma_p$ and occur in the vertical side walls. Stresses within the medium were mainly the same as the previous case with the same maximum compression of $1.336\,\sigma_p$. As there was not much change between the prestressed and reinforced concrete liners for dynamic loading, Figs. 5.7 and 5.8 are adequate to represent the change of stresses with time for the corresponding elements in the case of the prestressed concrete liner.

5.3.3.3 Active Rock Bolts

A wide spacing of rock anchors was used as shown in Fig. 5.11. The lengths of the anchors varied from 21 feet in the side walls to about 42 feet in the arched roof and the area of each anchor was $0.63\ in^2$ for a one-inch thickness in the perpendicular direction. The anchor pre-tension stress was 150 ksi.

i) *Static Loading*. The maximum inward horizontal displacement in the vertical walls was about 0.08 inch and the maximum vertical settlement of the arched roof was 0.119 inch. The two values are smaller than those for the unlined case by about 29% and 18% for Cases 1 and 2 respectively. The final deflected shape is shown in Fig. 5.12.

Owing to the prestressing forces in the rock anchors, stress concentrations around the anchors with a maximum compression of about 696 psi was found in the vertical and horizontal directions in different places. Tensile stresses were completely eliminated from the rock elements around the cavity. The stresses in the steel anchors ranged between 147,950 and

149,540 psi showing a decrease in prestress loss smaller than that for prestressed concrete. The area of steel anchors may be reduced and satisfactory results still will be obtained.

    ii) Dynamic Loading. The stresses within the rock media were higher than those in the case of reinforced or prestressed concrete liners. This may be due to the localized effect of the rock anchors and suggests the idea of using rock anchors in conjunction with any other liner type. However, this should be studied in relation to the total cost to obtain an economic design. The maximum recorded compressive stress was $1.694\sigma_p$ which is greater than the previous two cases, reinforced and prestressed concrete liners. The maximum tensile stress computed was $0.11\sigma_p$ in the vertical side walls of the cavity. This value was smaller than that for R.C. and P.C. liners due to the restraint offered by the rock anchors at this region.

    The stresses in the anchors were mainly tensile with a maximum of $14.4\sigma_p$. Only a few elements in the side faces were in compression with a maximum of $18.7\sigma_p$. The resulting tensile stresses should be taken into consideration during design as they increase the final tensile stresses in the anchors.

    Elements F, G and H in the medium and I, J and K of the anchors were chosen for studying the change of stress with time. Figs. 5.13a, b and c show stress-time relationships for the elements in the medium and Figs. 5.14a, b and c show the same relationships for rock anchors. Plotted on the figures are the stresses at the same locations for the dynamic loading treated as static one. The elements within the rock media behaved in the same manner as before but with smaller peak values of stresses. Stress reversal occurred in element G. Load factors of 1.25 and 1.6 were

obtained for elements F and G respectively. From the general stress field, a load factor ranging between 1.15 and 1.25 was obtained. In terms of design values, the stress reversal should be given special care as it can cause low cycle fatigue in the rock and steel anchors.

Stresses in the three anchors chosen changed from compression with small values to tension with high values. The corresponding static stresses were tensile with varying load factors of 1.45, 1.45 and 1.04 for the three anchors respectively.

5.3.3.4 Passive Rock Bolts

The same arrangement, as shown in Fig. 5.11, was used for studying passive rock bolting. The area of steel bars was increased to 1.89 in^2 which is three times that for active rock bolts. Passive rock bolts are not commonly used at present, so only comparative studies are restricted to static loading.

The maximum inward horizontal displacement in the vertical side walls was 0.119 inch and the maximum vertical settlement of the arched roof was 0.191 inch, which are approximately the same as those for the unlined case and consequently much higher than the values for active rock bolting. The final deformed shape of the cavity is shown in Fig. 5.12.

The general stress patterns around the cavity was kept almost the same as the unlined case. Only one element in the vertical side walls was under tension with a value of 28 psi. Almost all the steel bars were under tension with maximum values of 5039 psi at the middle of the vertical side walls.

5.3.3.5 Steel Liner

A steel plate of thickness 12 inch was used in this study. The

properties of the steel were assumed the same as those for the reinforcement of the concrete liner.

i) _Static Loading_. The maximum inward horizontal displacement of the side walls was 0.119 inch and the vertical settlement of the arched roof 0.172 inch. The horizontal displacement was almost the same as those for the unlined case while the vertical settlement was smaller by about 13%. The final deflected shape is shown in Fig. 5.15. The maximum normal stress in the steel liner was about 8500 psi. The largest magnitude of the tensile stresses in the rock adjacent to the steel liner was 66 psi which was almost the same as that for the unlined case.

ii) _Dynamic Loading_. The general stress pattern within the medium was almost as high as that in the case of the rock bolting. This may be due to the non-existence of a massive liner system. The maximum compression in the medium was $1.567\ \sigma_p$ which is slightly smaller than that for the case of the rock bolt lining. Very small values of tensile stresses in the medium were found with a maximum of $0.09\ \sigma_p$. A stress of about $7.3\ \sigma_p$ was obtained in the side walls of the steel liner. The variations of stress with time have been plotted in Figs. 5.16a, b and c for the medium at locations L, M and N. The variation of bending moment with time have been plotted for nodes 1 and 2 in Figs. 5.17a and b (nodes 1 and 2 are shown in the same figure). Plotted on the same figures are the corresponding static values. A load factor of about 1.1 was found for element L and stresses changed from compression to tension at location M with a high tensile stresses in dynamic $(0.45\ \sigma_p)$ than the static tensile stress $(0.169\ \sigma_p)$. For all types of liners, the location at element N gave a static stress value equal to the dynamic value. At nodes 1 and 2, the stresses increase with time and a dynamic load factor of 1.2 was found.

5.4 Thermal Stresses

The stress distribution within the medium and the liner was studied considering only two cases, prestressed concrete and active rock bolt lining. Within the studied region a temperature gradient from 150°F at the interior face of the cavity to zero at the boundary was assumed. Coefficients of thermal expansion of 5.5×10^{-6} in/in.F° for concrete and steel and 4×10^{-6} in/in.F° for rock were assumed.

5.4.1 Prestressed Concrete Liner

Figs. 5.18a and b show the horizontal and vertical stress distributions along two vertical and horizontal sections. In general, all the stresses are in compression. In Fig. 5.18a the horizontal stresses decrease gradually with distance from the cavity. The rate of change is very high within few feet from the cavity face. This may be due to the effect of the steel reinforcement at the interior face. A maximum horizontal stress value of 2930 psi occurred at the crown of the arch. The maximum value in the horizontal section was 1660 psi. In Fig. 5.18b the horizontal section showed a gradual decrease in the vertical stresses with a maximum value of about 1920 psi. Along the vertical section the vertical stresses increased from zero at the crown of the arch to a maximum of 718 psi near the end and then decreased slightly towards the upper boundary.

The concrete liner around the cavity was subjected to high tensile stresses, particularly in the vertical side walls with a maximum value of 263 psi. Stresses in the steel reinforcement were compressive with high values ranging between 27,700 and 36,600 psi. These values correspond to 18.4% and 24.4% loss of prestress.

5.4.2 Active Rock Bolts

Figs. 5.19a and b show the horizontal and vertical stress distributions. The stresses are mainly compressive but less in magnitude than those for the prestressed liner. Almost similar stress gradients were obtained but with no relative high values at the face of the cavity. The maximum horizontal stresses in the vertical and horizontal sections were 1750 and 1050 psi while the maximum vertical stresses were 745 and 1345 psi respectively. Some tensile stresses were found around the cavity with maximum of 226 psi. The stresses in some steel anchors were compressive with maximum value of 23,600 psi, and in the others were tensile with low values of maximum 5180 psi. These values correspond to a maximum loss of prestress of 15.7% and a maximum gain of prestress of 3.5% respectively.

5.5 Comparative Study

The intent of any structural design is to find the structural system that functions and gives minimum straining action under the effect of the operating loads. This can be achieved by trial and error. In the underground cavities different shapes and different types of liners are assumed and subjected to the operating loads. Displacements and stresses are obtained for each case and compared with other cases. On the basis of these comparisons a particular type can be chosen and modified for better results and studied again. Depending on the results other modifications can be suggested and the iteration repeated. Finally, a reasonable shape with a suitable lining type is obtained. Ease of analysis depends mainly on the available techniques used.

In this study, a practical shape was assumed and five types of liners were studied. The operating loads considered were the in-situ

stresses including the deadweight of the rock, dynamic loading resulting from nuclear explosions and temperature effects.

Rock resists mainly compressive stresses and one of the functions of a reasonable liner is to minimize the tensile stresses. Also, the other functions are to reduce displacements of the cavity sides and to ensure that the compressive stresses within the surrounding media are low. The importance of costs and the availability of the lining materials are obvious but outside the scope of this thesis.

It was expected that the prestressed concrete liner would satisfy some of these requirements but the two cases considered gave higher values of displacements with tensile stresses in the cavity walls. Under the temperature effect a high loss of prestress occurred and a high stress concentration was introduced around the cavity due to the effect of the prestressed steel.

Displacements resulting from the case of reinforced concrete liner were reasonable but the tensile stresses were still there. Stress reversal under dynamic loading causes fatigue which reduces the strength of any lining material, particularly in the case of the concrete liner.

Passive rock bolting was not effective in decreasing the displacements or stresses and tensile stresses could not be eliminated. It is expected that this type of liner is structurally effective only if the rock is liable to slide which is a special case.

The stress values obtained for the 12 inch steel plate lining were almost the same as those for the case of the reinforced concrete liner and the stresses within the rock around the cavity were relatively high.

Active rock bolting type gave fairly good results in reducing both the displacements of the cavity sides and the stresses in the surrounding

rock. The loss of prestress due to elastic compression of rock was less than that for the prestressed concrete liner and the behaviour of the bolts under the temperature effect was better. The idea of using other liner types such as a R.C. liner in conjunction with the rock bolting may improve the drawbacks resulting from using the active rock bolting alone but the costs should be given careful consideration.

5.6 Conclusions

1. Active rock-bolting gave the best results by decreasing displacements and eliminating tensile stresses in the walls. Its behaviour under the temperature effect was better. The design of anchors should take into consideration the tensile stresses resulting from the dynamic loads.

2. This study assumed ideal conditions in rock with no joints or sliding. The static stresses obtained were far below the actual strength of the rock or lining material. So the design based on these stresses alone will give small thicknesses of liner cross-sections and consequently it will be unsafe design. Hence, for the safety of the structure, the design should be based on the combined stresses resulting from the static load and any expected dynamic loading.

3. A dynamic load factor in the range between 1.15 and 1.25 is reasonable for preliminary design but special consideration should be given to stress reversals, particularly, if the dynamic loading is repetitive. This causes fatigue for the lining material and cannot be predicted by the static application of the dynamic load values. A reasonable factor of safety taking fatigue into account should be assumed based on the available codes of practice.

4. The steel reinforcement and anchor bolts showed load factors higher than 1.25 indicating the need for different load factor. From the results obtained a factor of 2 would be reasonable.

5. The thermal stresses were very high compared with those for the dead-weight of the rock. Temperature stresses should therefore be computed based on the probability of occurrence of the temperature gradient under operating conditions.

6. The results obtained for the prestressed concrete liner were not reasonable.

5.7 Recommendations for Further Study

1. The actual properties of the rock such as anistropy, elasticity and low tensile strength should be considered. The same holds true for the lining material.

2. The problem of simulating an infinite medium should be given careful consideration. The proper simulation should be suitable for both static and dynamic analysis.

3. In the case of the prestressed concrete liner, the study should be extended to include the consideration of a reasonable tendon profile, area of prestressed steel and the value of prestress that would give better stress redistribution around the cavity. The methods of prestressing underground should be included in the study.

4. The substructuring technique as presented by Atchison (2) and Liaw and Chopra (18) is best suited for this case. Adoption of this method will facilitate computation of the medium stresses using plane strain analysis while the stresses in the linings can be obtained using three-dimensional analysis.

5. The results of this analysis may be improved by considering linear strain quadrilateral elements.

TABLES AND FIGURES

Project	Rock Type	Length (feet)	Shape
Pumping Chamber at Lake Mead	Hard quartz-biotite gneissic chest and granite-gneiss	122	
The Churchill Falls Underground Powerhouse	Diorite-gabbro, granite, seynite and pegmatite	972	
Power Plant Chamber Under Orville Dam	Metamorphic rock and granite	550	
Mica Project	Mica chist and granitic paragneiss	1950	
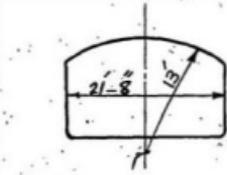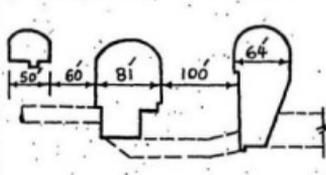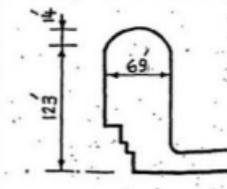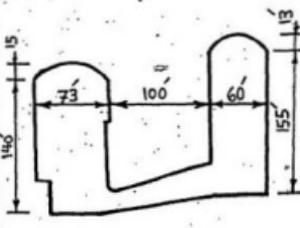
Table 2.1. Typical shapes of underground power plants

Table 3.1 Summary of Several Recommendations
of Time Interval for Numerical
Integration (Ref. 6)

Author	$T_{min}/\Delta t$
Levy	30
Newmark	depends on method of integration
Costantino	5
Namyet	6
Biggs	6-10
Agbabian	10
Lycan	variable
Wilson	depends on desirability of excluding higher modes
Wang	40
Timoshenko	24
Salvadori	4
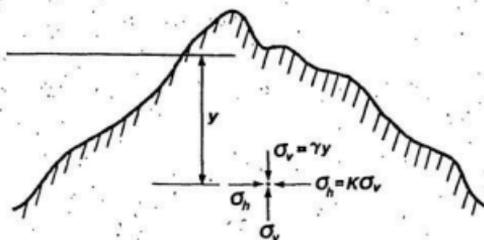
Fig. 2.1 Stressing of a point in all directions

(a) $\sigma_{td} > 2p$ (b) $\sigma_{td} < 2p$ (c) Crushed rock
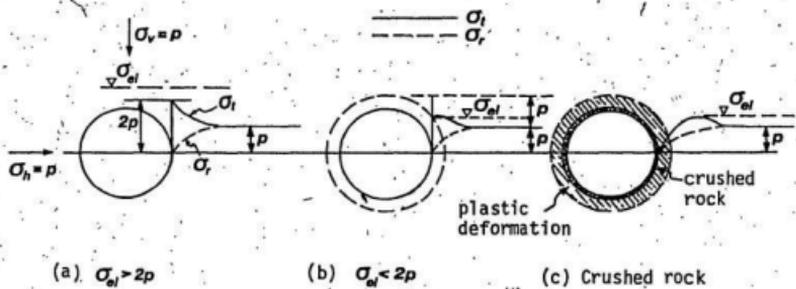
Fig. 2.2 Stresses around cavities in isotropic rock.
Uniform residual stress($\sigma_v = \sigma_h = p$) (Ref. 11)
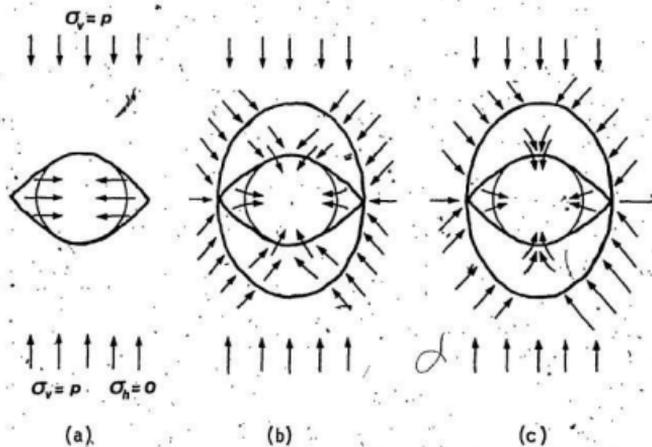
Fig. 2.3 Stresses and strains around a cavity in rock.
Initial residual stresses uniaxial(Ref. 11)

M = 0

For very shallow depths or for openings near vertical rock surfaces

$\sigma_H = 0$
$\sigma_v = \gamma H$

M = $\frac{1}{3}$

For larger range of depths

$\sigma_H = \frac{1}{3}\sigma_v$
$\sigma_v = \gamma H$

M = 1

For great depths

$\sigma_H = \sigma_v$
$\sigma_v = \gamma H$
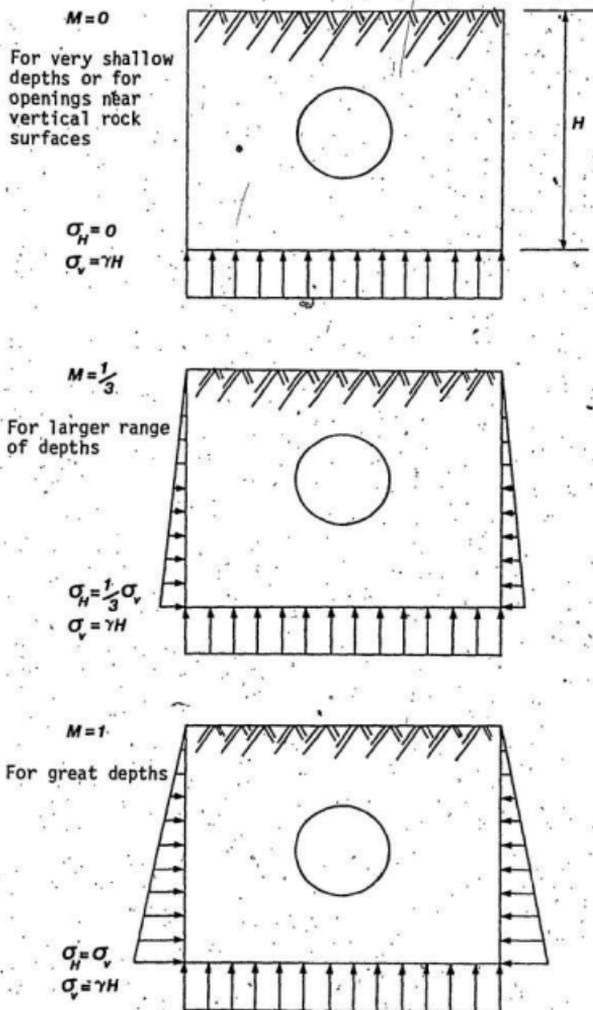
Fig. 2.4 Three assumed types of stress fields(Ref. 6)

66

Fig. 2.5 Two-element bar

Poisson's ratio $\nu = 0.3$
Cavity radius $R = 40$ ft
Rock density $\rho = 150$ pcf

Lithostatic

Internal
Pressure

Combined stress

Depth

Tension

Compression
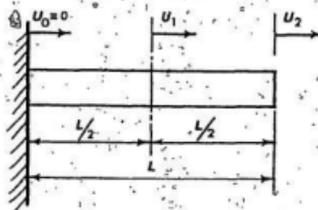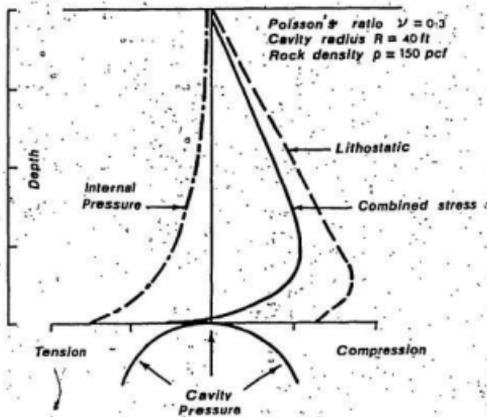
Cavity
Pressure

Fig. 2.6 Stress distribution above pressurized
cylindrical cavity.(Ref. 33)
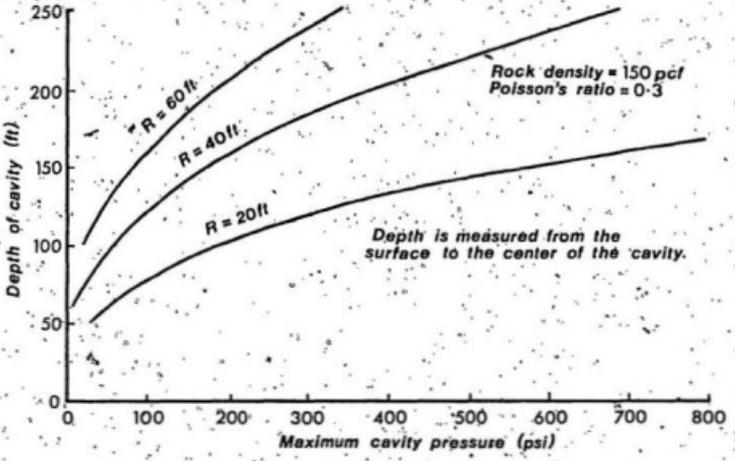
Fig. 2.7 Cavity depth vs pressure(cylindrical cavity)   (Ref. 33)

(R - radius of the cavity)
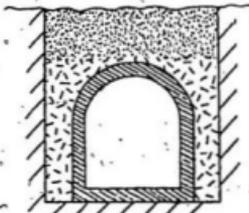
(a) Cut and cover in rock or soil
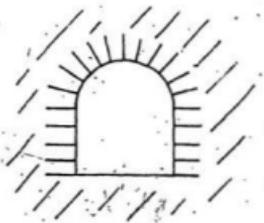
(b) Unlined cavity in rock
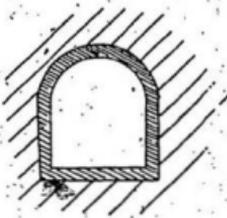
(c) Lined cavity in rock or soil
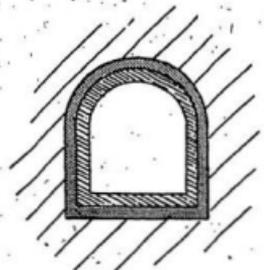
(d) Lined cavity in rock or soil with annular filling of soft material
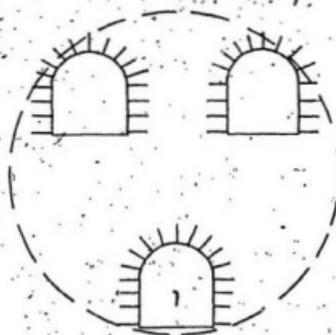
(e) Multiple cavities

Fig. 2.8 Underground cavities (Ref. 33)
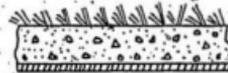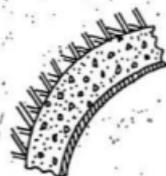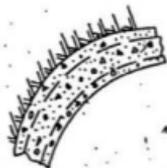
(a) Reinforced concrete liner

(b) Composite liner

Fig. 2.9 Liner type (Ref. 33)
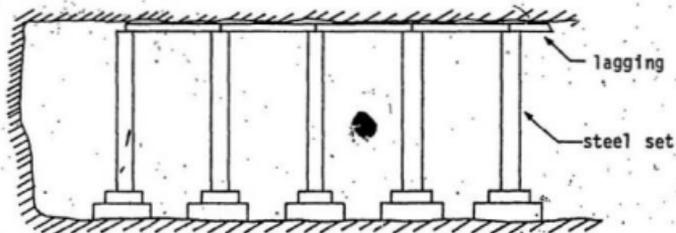
Fig. 2.10 Steel-rib tunnel support (Ref. 25)
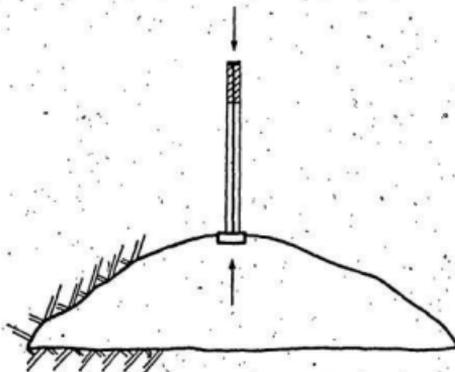
(a) Roof support
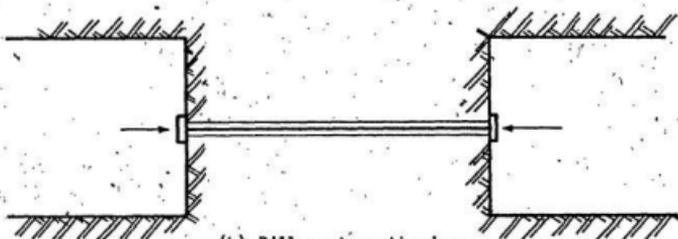
(b) Pillar strengthening
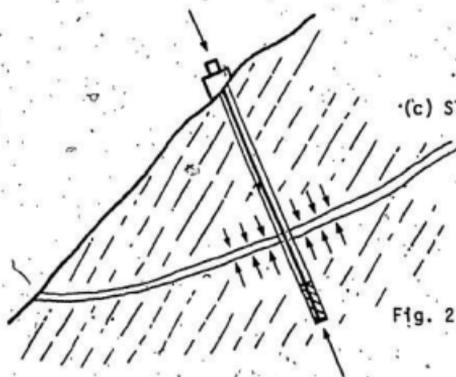
(c) Slope stabilization

Fig. 2.11 Some uses of rock anchors (Ref. 7)
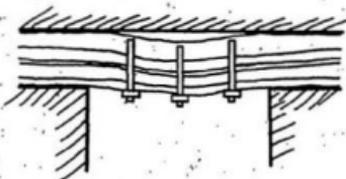
Fig. 2.12 Roof supported by bolting
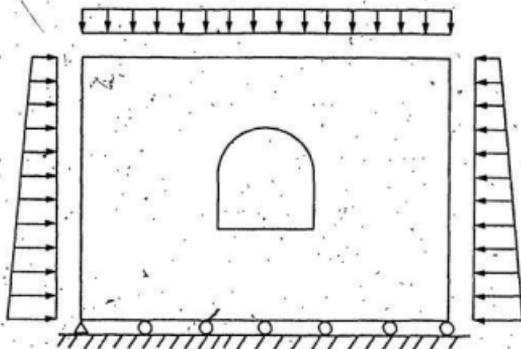
Fig. 3.1 Boundary conditions for simulation
of in-situ stresses (Ref. 4)
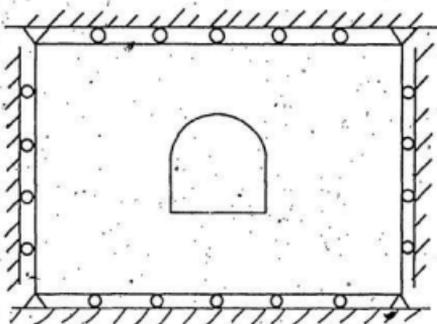
Fig. 3.2 Alternative simulation of boundary
conditions for in-situ stresses(Ref. 4)
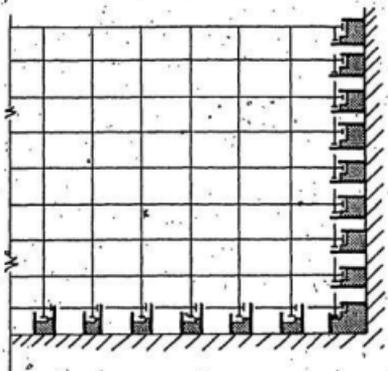
Fig. 3.3 Finite element model with energy
absorbing boundary conditions(Ref. 19)
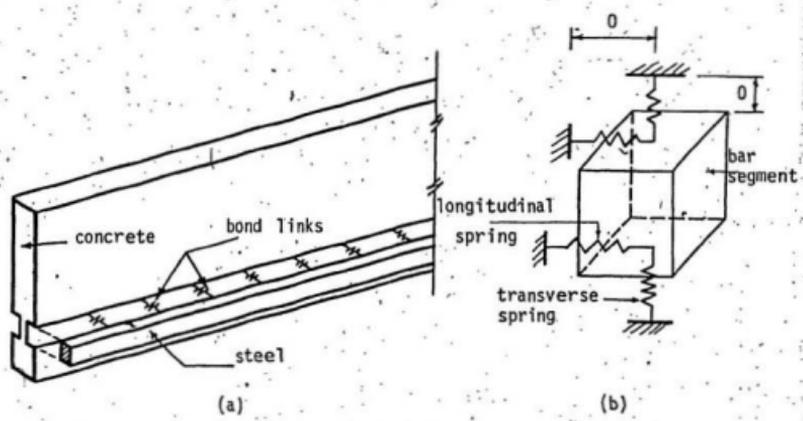
Fig. 3.4 Details of bond linkage
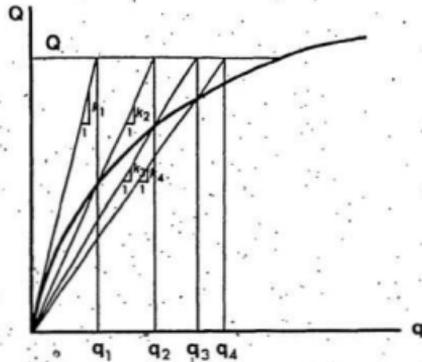
(a) Variable stiffness method
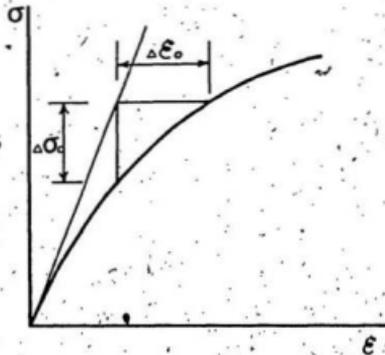
(b) Initial stress and initial strain processes

Fig. 3.5 Elastic-plastic behaviour
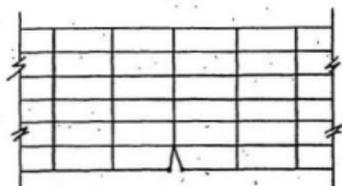
(a) Edge crack
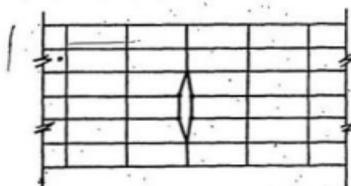
(b) Interior crack
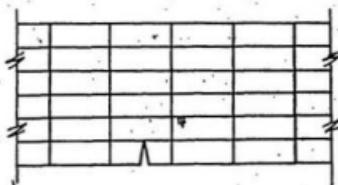
(c) Separation within the element

Fig. 3.6 Representation of cracks in physical models

(a) local axes

(b) Transformation of axes
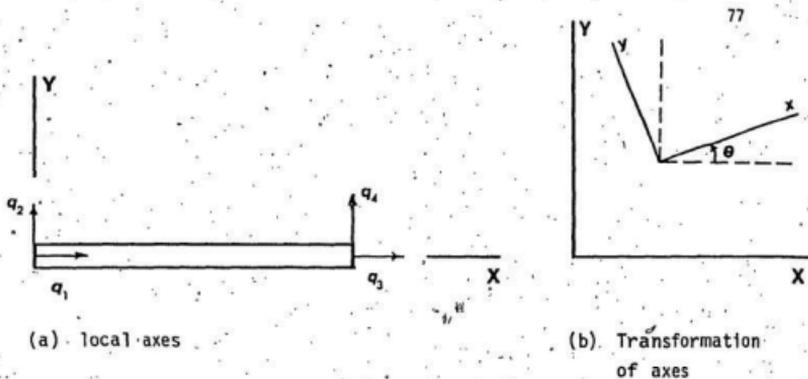
Fig. 3.7 Bar element-degrees of freedom in local coordinates
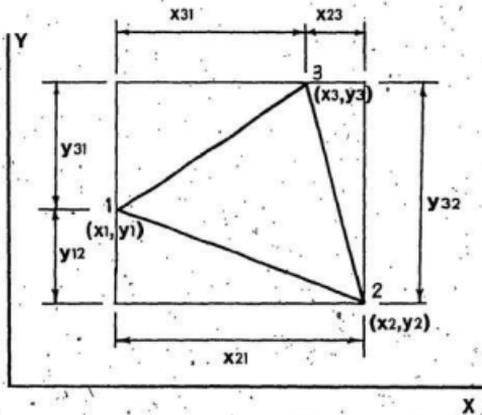
Fig. 3.8 Triangular element
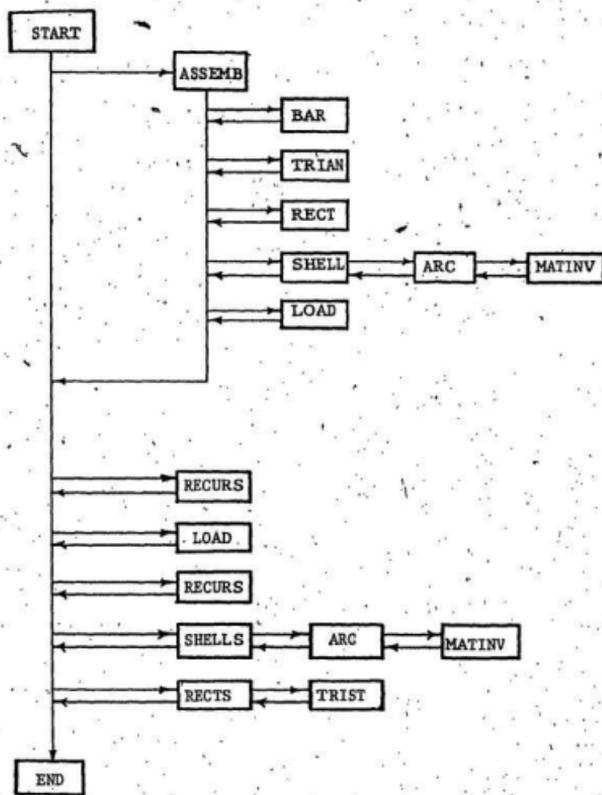
Fig. 4.1 Flow-chart for Blakey's programme (Ref. 6)
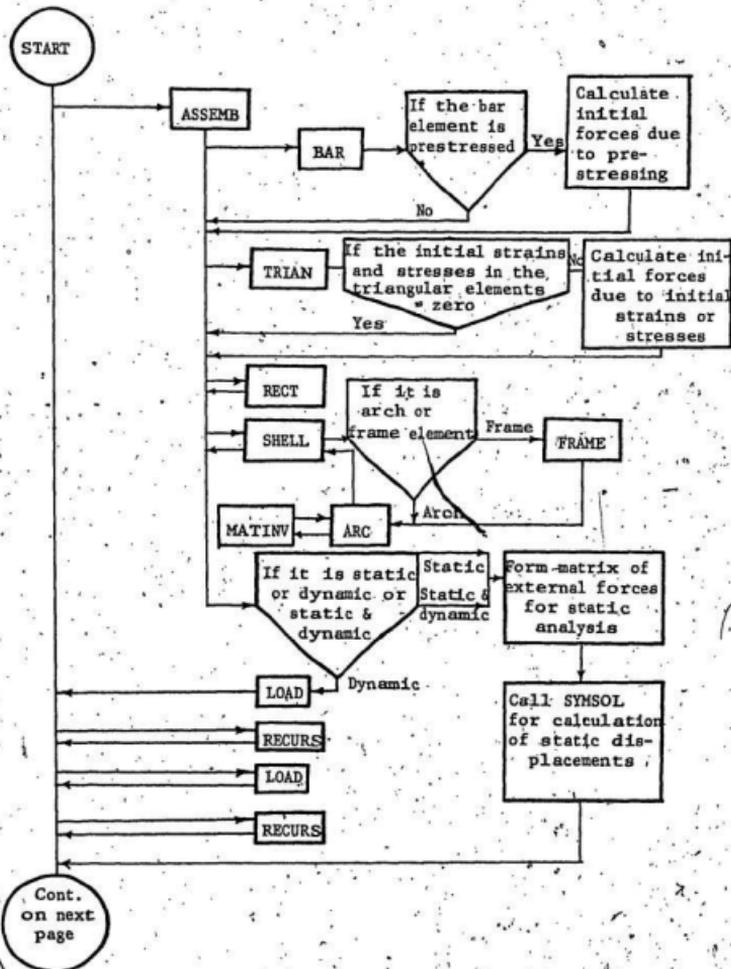
Fig. 4.2 (continued on the next page)
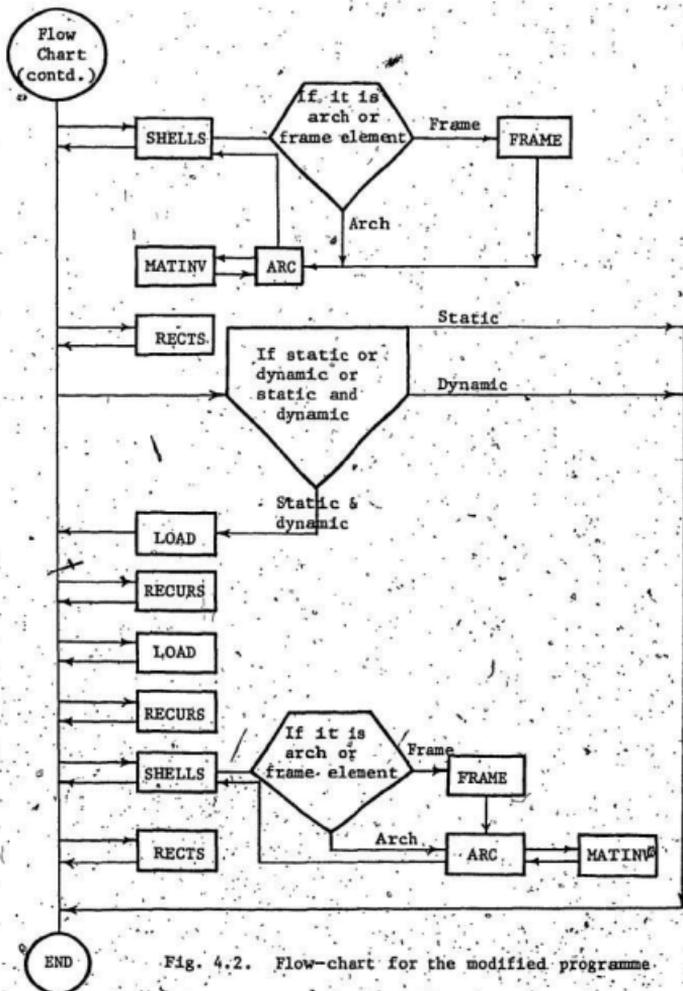
Fig. 4.2. Flow-chart for the modified programme
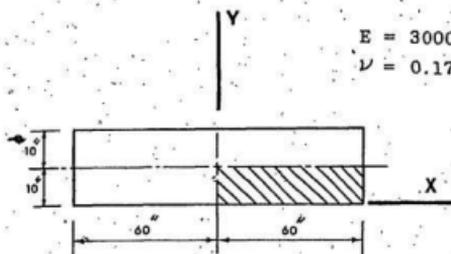
Fig. 4.3a Test problem
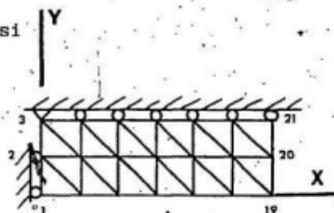
Fig. 4.3b Finite element mesh

$E = 3000$ ksi
$\nu = 0.17$
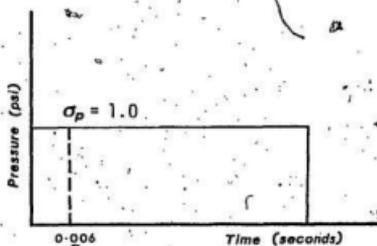
Fig. 4.4 Load-time function for
the test problem
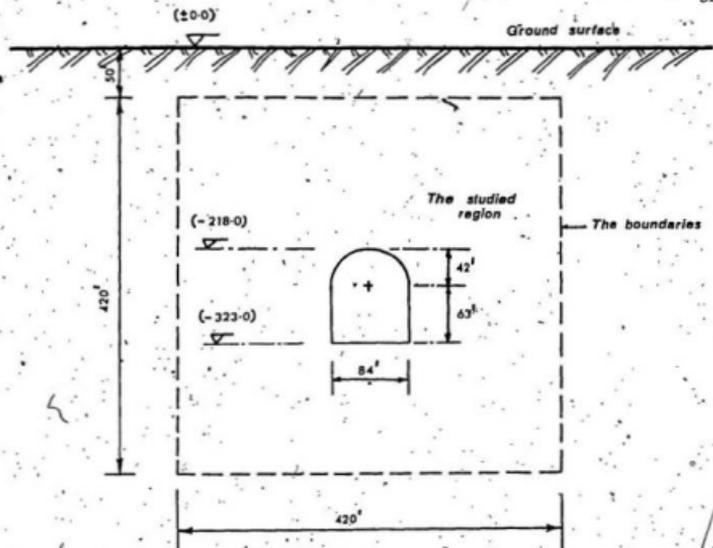
Fig. 5.1. The studied cavity
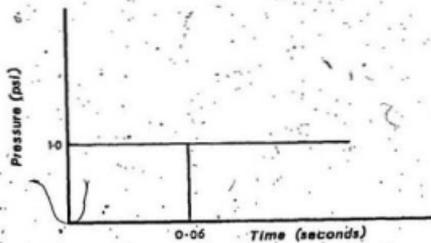
Fig. 5.2 Applied dynamic load ($\sigma_p^- = 1.0$ psi)
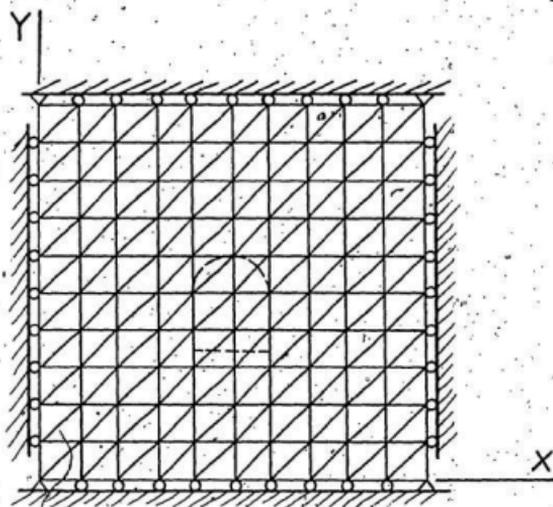
Fig. 5.3 Mesh used for in-situ stress determination

No. of nodes ....= 120
No. of elements ....= 200
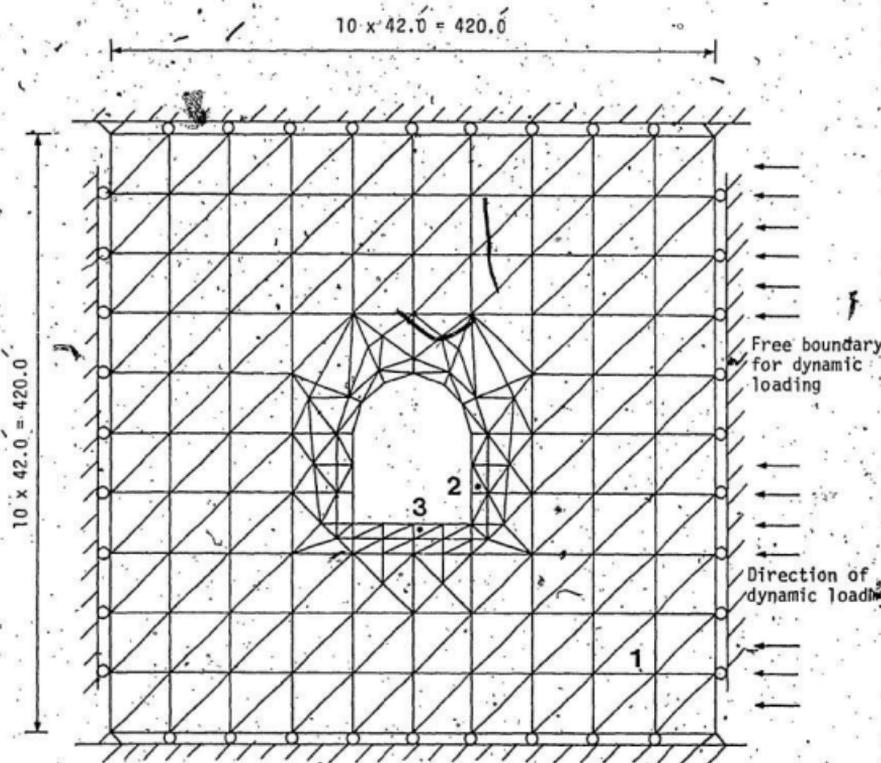
Fig. 5.4a Mesh used for determination of induced stresses

No. of nodes ....= 168
No. of elements ....= 280

Scale:

for deformation 5:1
for shape 1:7
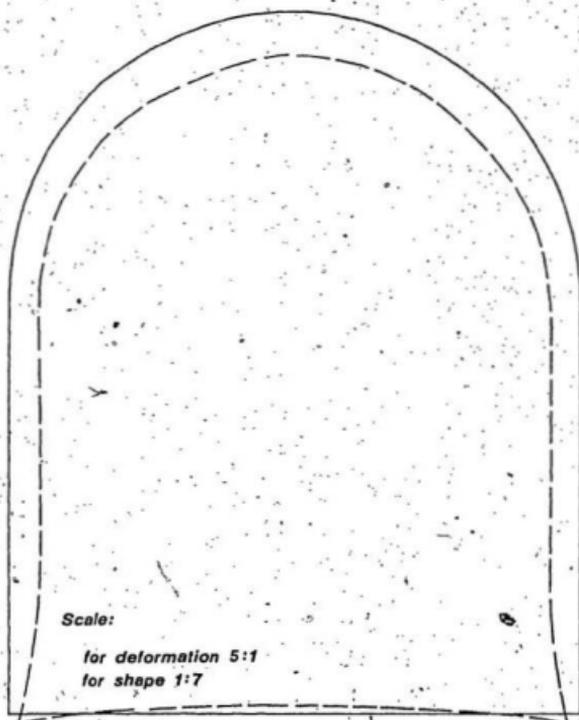
Fig. 5.4b The deformed shape under deadweight of rock
(Unlined cavity)
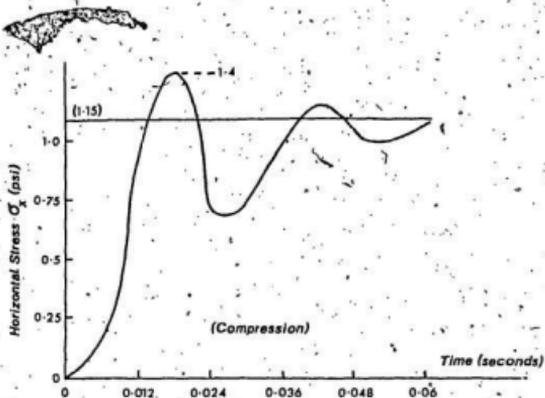
Fig. 5.5a Stress vs time for element 1
(Unlined cavity)
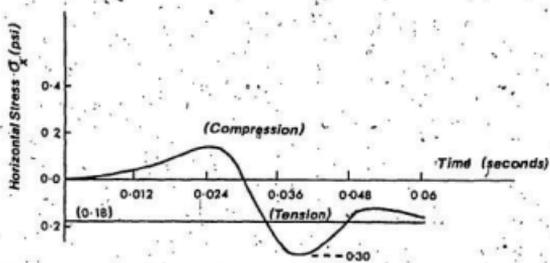
Fig. 5.5b Stress vs time for element 2(Unlined cavity)
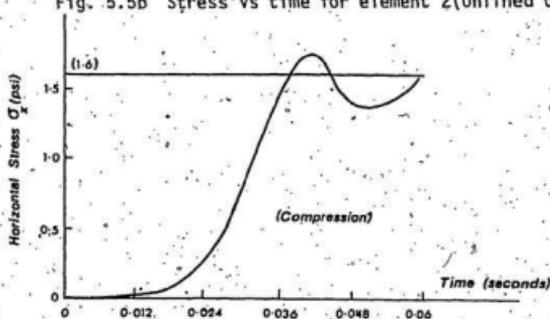
Fig. 5.5c Stress vs time for element 3(Unlined cavity)
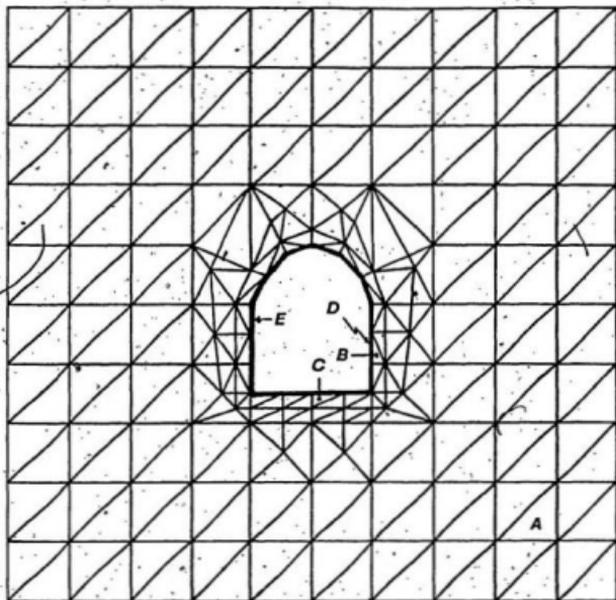
Fig 5.6 Mesh used in case of R.C. liner

No. of nodes ....= 168
Total No. of elements ....= 296
No. of steel elements ....= 16
Area of each steel element ......= 1.89 in^2
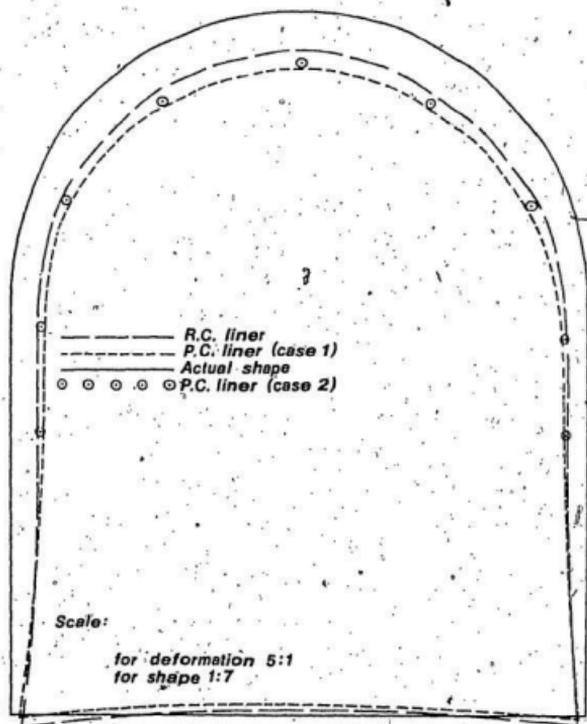
Fig. 5.7 The deformed shape under deadweight of rock
(R.C. and P.C. liners)
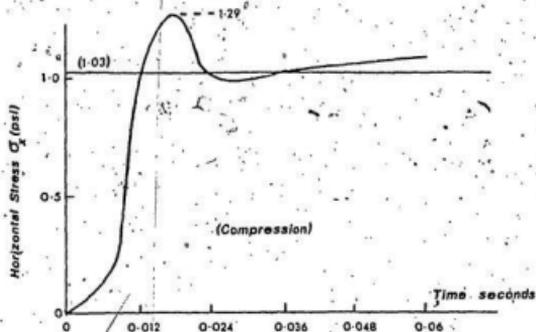
Fig. 5.8a Stress vs time for element A(R.C. liner)
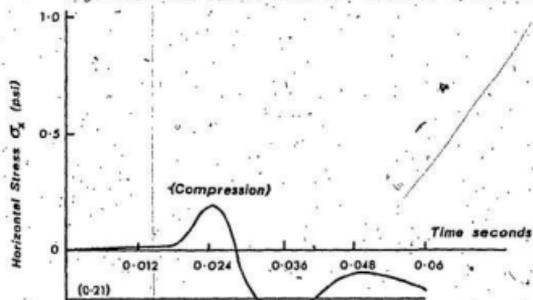
Fig. 5.8b Stress vs time for element B(R.C. liner)
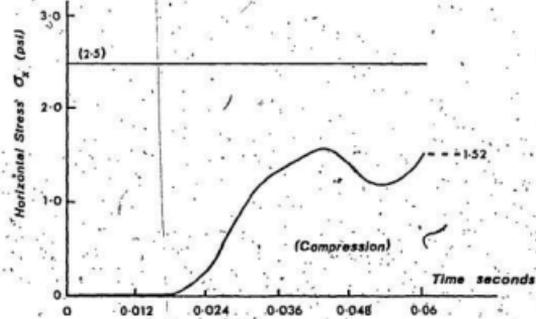
Fig. 5.8c Stress vs time for element C(R.C. liner)
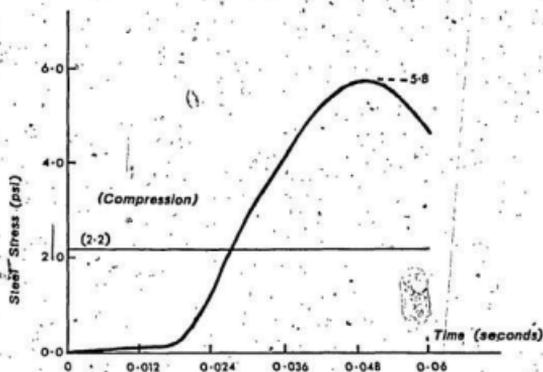
Fig. 5.9a Stress vs time for element D(R.C. liner)
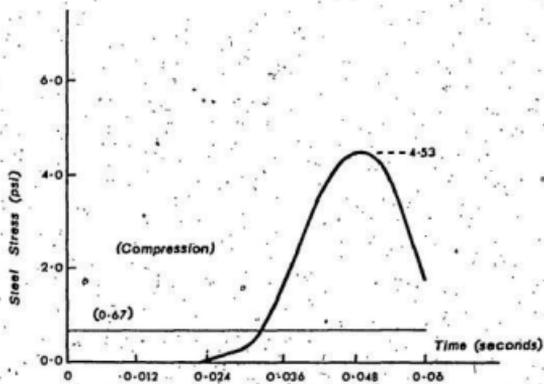
Fig. 5.9b Stress vs time for element E(R.C. liner)
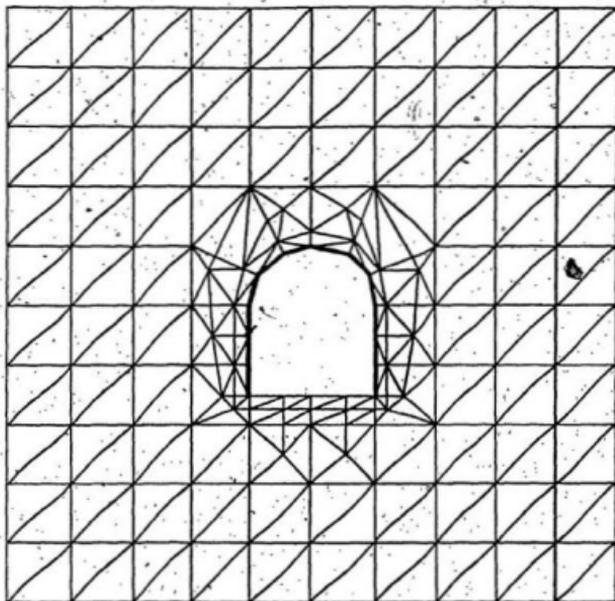
Fig. 5.10a Mesh used in Case 1 for P.C. liner

No. of nodes ....= 168
Total No. of elements ....= 292
No. of prestressed steel elements ....= 12
Area of each steel element ....= 0.63 in^2
Initial prestress ..=150 ksi
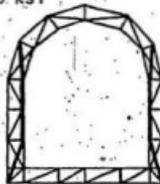
Fig. 5.10b Tendon profile for Case 2
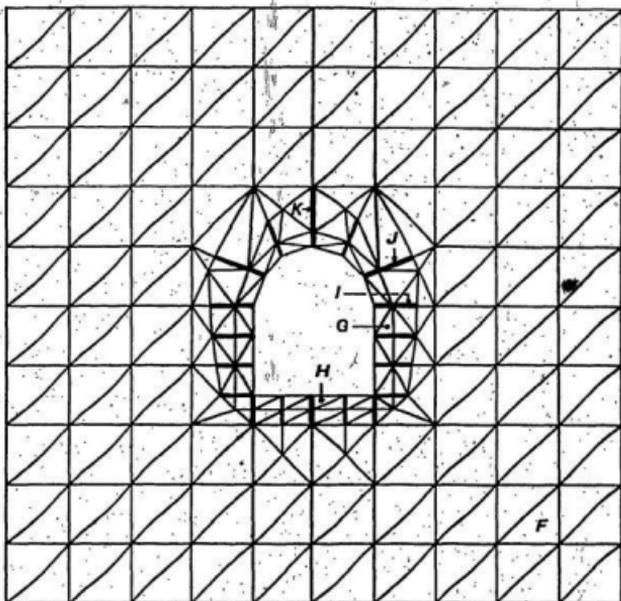
Fig. 5.11 Mesh used in case of rock bolting.

No. of nodes ....= 168
Total No. of elements ....= 316
No. of steel anchors ....= 36
Area of each anchor ....= 0.63 in^2
Initial prestress ....= 150 ksi

Active rock bolt
Passive rock bolt
Actual shape

Scale:

for deformation 5:1
for shape 1:7
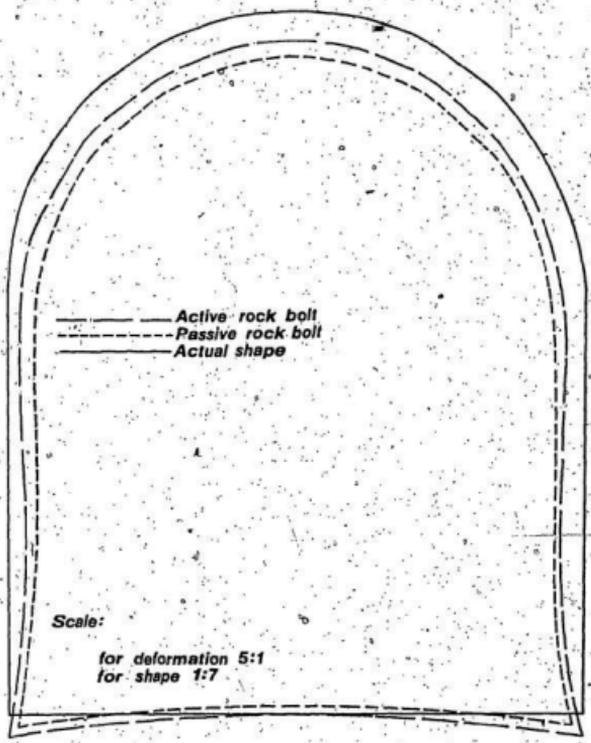
Fig. 5.12 The deformed shape under deadweight of rock.
(Active and passive rock bolting)
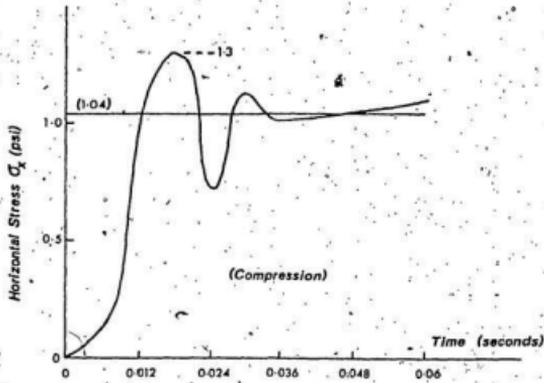
Fig. 5.13a Stress vs time for element F
(Active rock bolting)
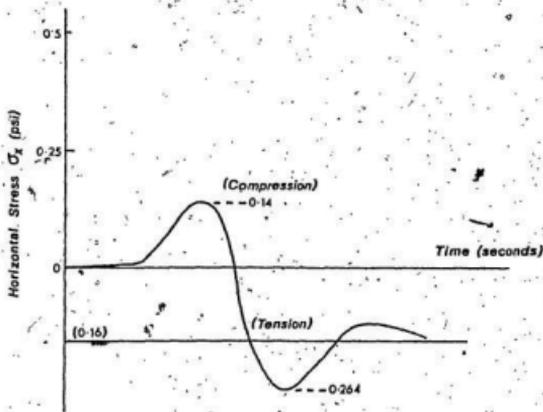
Fig. 5.13b Stress vs time for element G
(Active rock bolting)
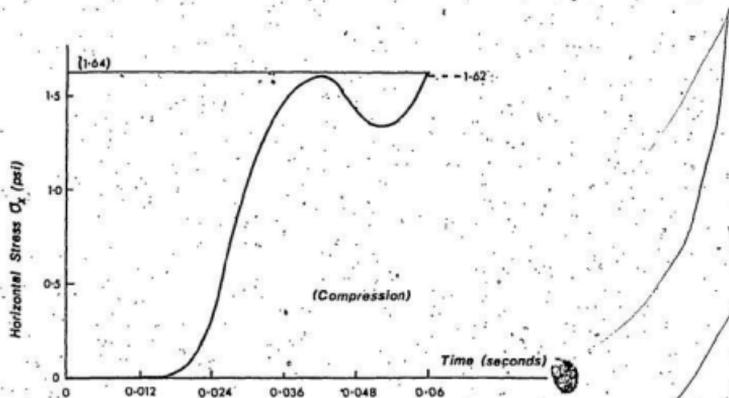
Fig. 5.13c Stress vs time for element H
(Active rock bolting)
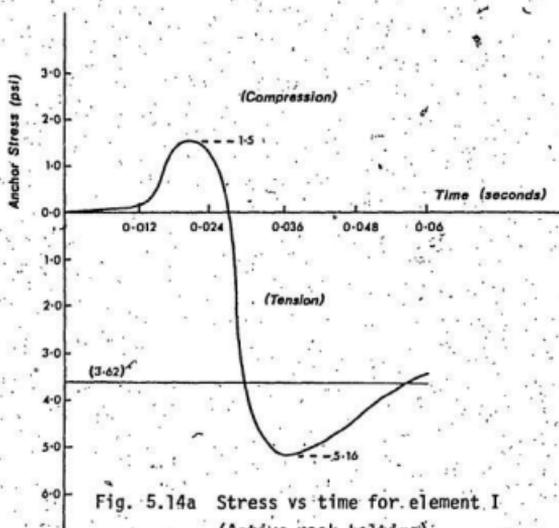
Fig. 5.14a Stress vs time for element I
(Active rock bolting)
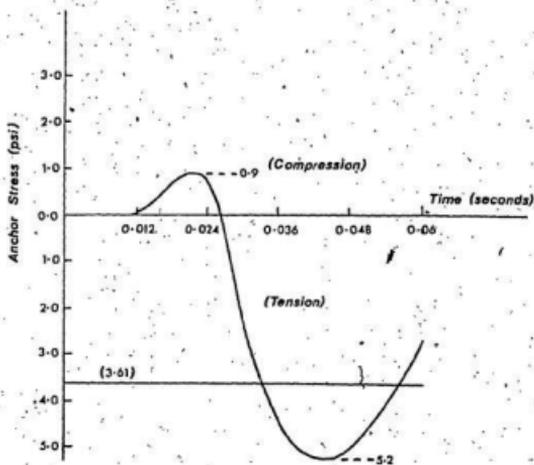
Fig. 5.14b Stress vs time for element J.
(Active rock bolting)
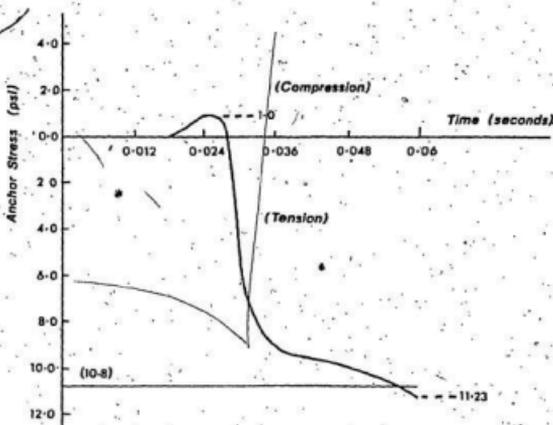
Fig. 5.14c Stress vs time for element K (Active rock bolting)

Scale:

for deformation 5:1
for shape 1:7
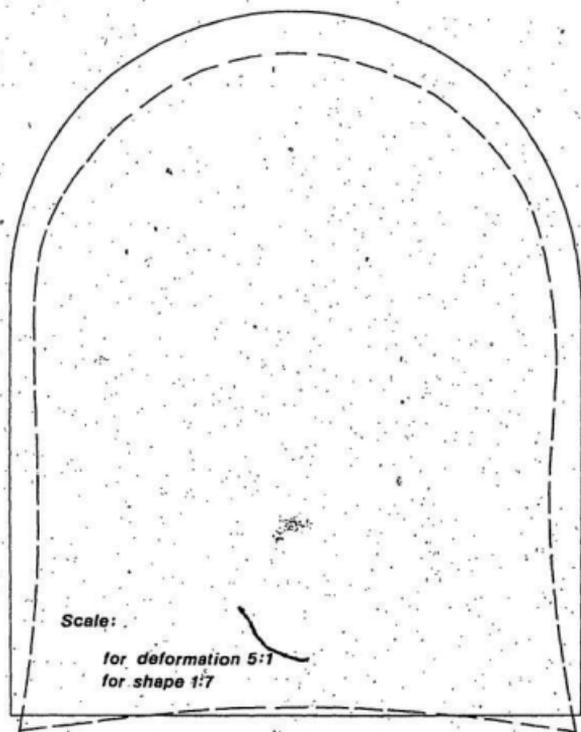
Fig. 5.15 The deformed shape under deadweight of rock
(Steel liner)
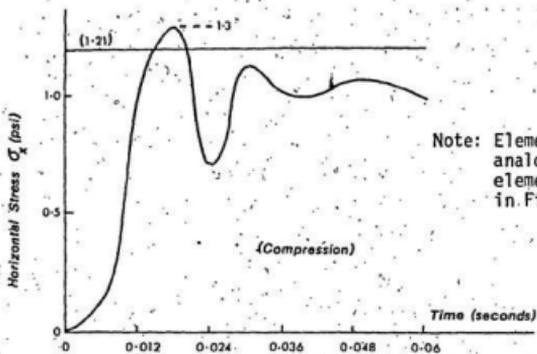
Fig. 5.16a Stress vs time for element L(Steel liner)

Note: Elements L,M&N are analogous to elements A,B&C indicated in Fig. 5.6
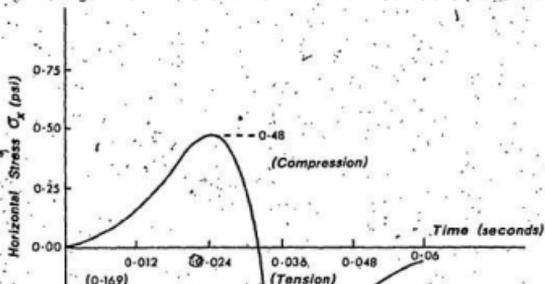
Fig. 5.16b Stress vs time for element M(Steel liner)
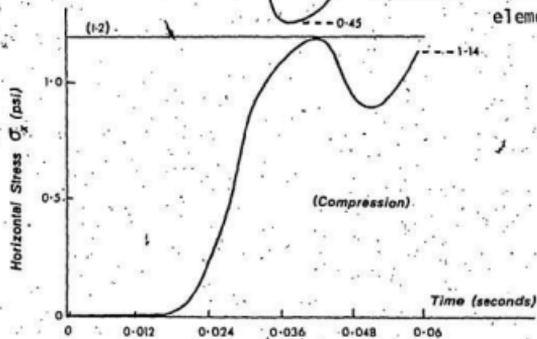
Fig. 5.16c Stress vs time for element N(Steel liner)
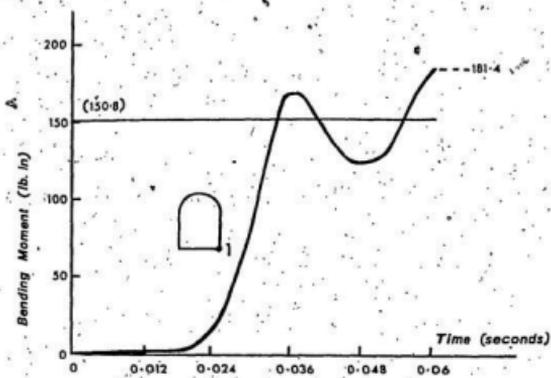
Fig. 5.17a Bending moment vs time at node 1
(Steel liner)
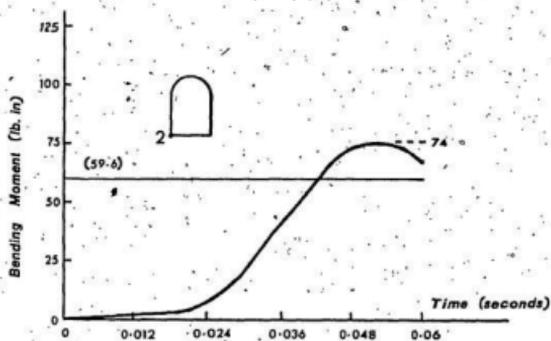
Fig. 5.17b Bending moment vs time at node 2
(Steel liner)
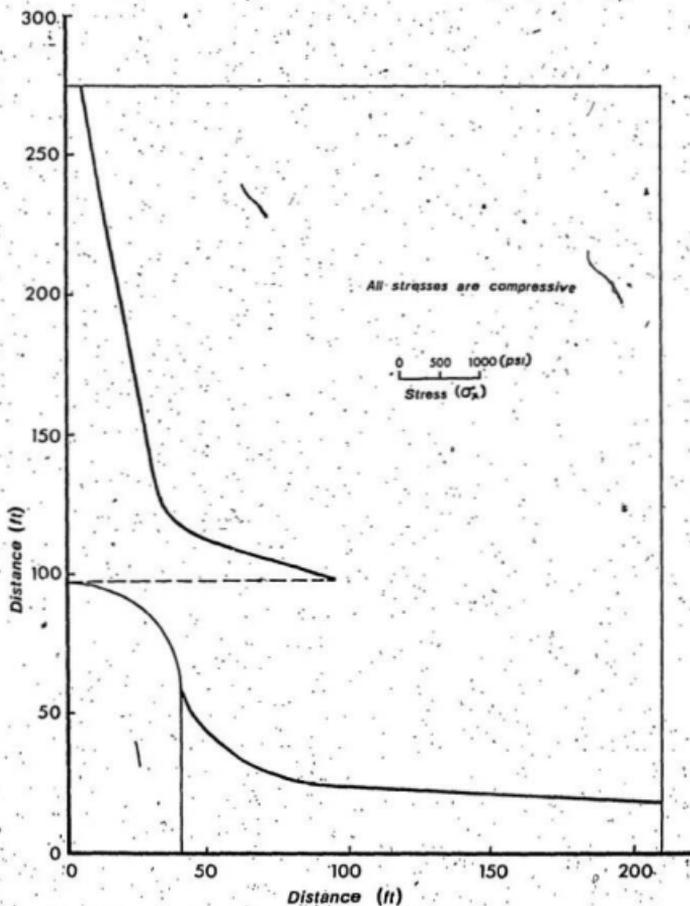
Fig. 5.18a Horizontal stress (σ_x) distribution due to temperature gradient from 150°F at the cavity face to zero at the end of the region (P.C. liner)
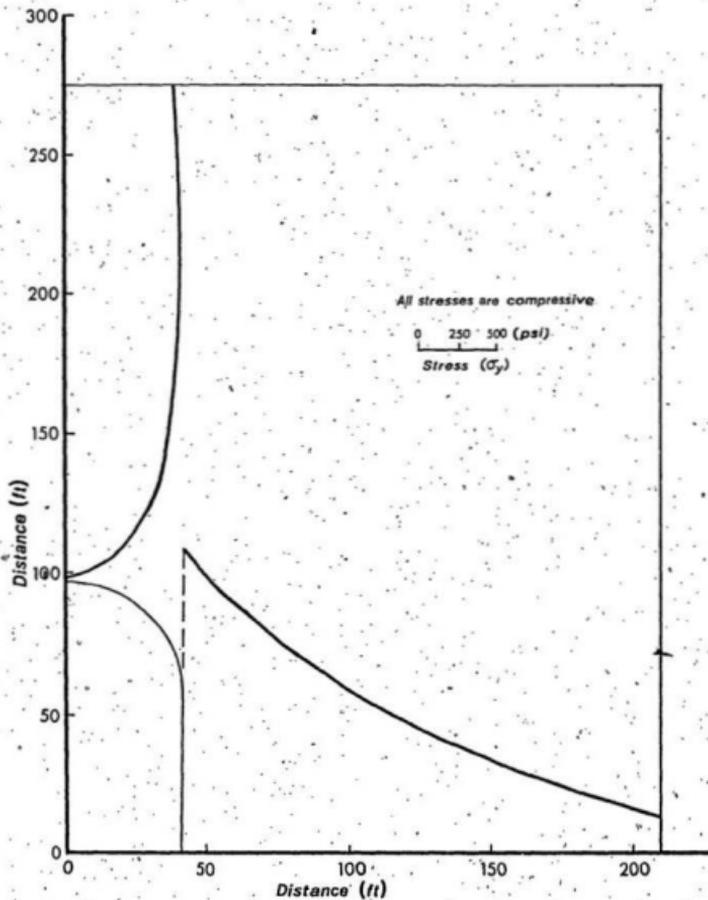
Fig. 5.18b Vertical stress(σ_y)distribution due to temperature
gradient from 150°F at the cavity face to zero at
the end of the region(P.C. liner)
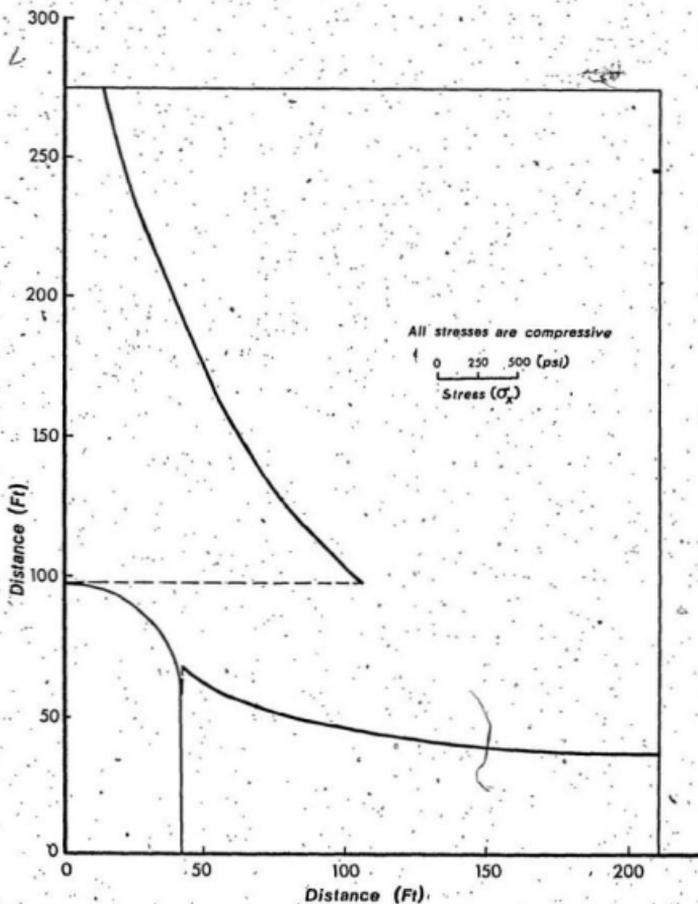
Fig. 5.19a Horizontal stress(σ_x)distribution due to temperature
gradient from 150°F at the cavity face to zero at the
end of the region(Active rock bolting)
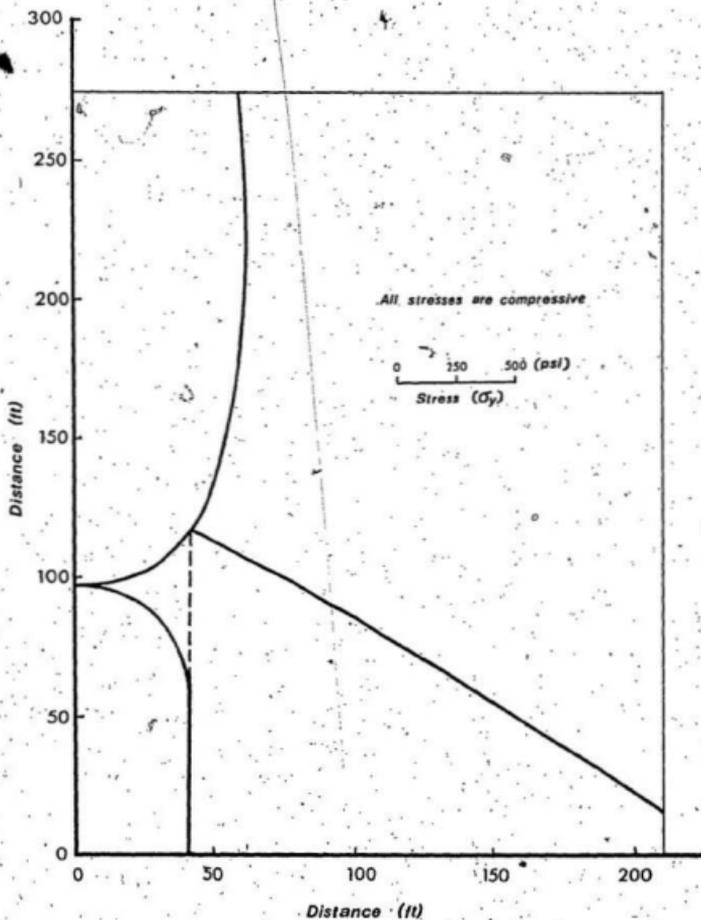
Fig. 5.19b Vertical stress(σ_y)distribution due to temperature gradient from 150 F at the cavity face to zero at the end of the region(Active rock bolting)

REFERENCES

REFERENCES

1. Allgood, J. R. "Summary of Soil-Structure Interaction." Naval Civil Engineering Laboratory, Technical Report R-771, Port Hueneme, California (July 1972).

2. Atchison, D. L. "Finite Element Solution of the Interaction of Plane Acoustic Blast Wave and a Cylindrical Structure." M. Eng. Thesis, U. S. Naval Postgraduate School. (1974).

3. Bender, M. "A Status Report on Prestressed Concrete Reactor Pressure Vessel Technology." Parts I and II. Nuclear Structural Engineering, 83-90 and 206-223 (1965).

4. Benson, R. P., Kierans, T. W., and Sigvaldson, O. T. "In-situ and Induced Stresses at the Churchill Falls Underground Powerhouse, Labrador." Second Congress of the International Society of Rock Mechanics, Belgerade, Yugoslavia (Sept. 1970).

5. Benson, R. P., Conlon, R. J., Merritt, A. H., Joli-Coeur, P., and Deere, D. U. "Rock Mechanics at Churchill Falls." ASCE Symposium on Underground Rock Chambers, Phoenix, Arizona, 407-486 (1971).

6. Blakey, L. H. "Dynamic Response of Reinforced Openings in Rock." Ph.D. Thesis, The Catholic University of America (1971).

7. Coates, D. F., and Sage, R. "Rock Anchors in Mining - A Guide for Their Utilization and Installation." Special Publication, Dept. of Energy, Mines and Resources, Ottawa, Canada (November 1973).

8. Cording, E. J., Hendron, A. J., and Deer, D. R. "Rock Engineering for Underground Caverns." ASCE Symposium on Underground Rock Chambers, Phoenix, Arizona, 567-600 (1971).

9. Desai, C. S., and Abel, J. F. "Introduction to the Finite Element Method." Van Nostrand Reinhold Company (1972).

10. Goodman, R. E., and Ewoldsen, H. M. "A Design Approach for Rock Bolt Reinforcement in Underground Galleries." Int. Symposium on Large Permanent Underground Openings, Oslo, Norway, 181-195 (1969).

11. Jaeger, C. "Rock Mechanics and Engineering." Cambridge at the University Press (1972).

12. Jaeger, T. A. "Note on Stress Analysis of Prestressed Concrete Reactor Pressure Vessels." Nuclear Structural Engineering, 133-136 (1965).

13. Kierans, T. W., Reddy, D. V., and Heale, D. G. "Engineering Methods for Seismic Design of Nuclear Plant Facilities." Manual Item 11.1 Underground Facilities, Prepared for the Approval of the Seismic Task Group of the ASCE Committee for Nuclear Engineering and Materials (July 1974).

14. Kierans, T. W., Reddy, D. V., and Heale, D. G. "Dynamic Analysis and Structural Design of Primary Underground Nuclear Facilities." Draft for the Seismic Nuclear Facilities, Meeting at Atlanta, Georgia (October 1973).

15. Kripanarayanan, K. M., and Meyers, B. L. "Transfer Stress Distribution Using the Finite Element Method." Symposium on Finite Element Method, McGill University (1970).

16. Kuhlemeyer, R. L., and Lysmer, J. L. "Finite Element Method Accuracy for Wave Propagation Problems." Proceedings of the ASCE, Soil Mechanics and Foundation Division, Vol. 99, No. SM5, 421-427 (May 1973).

17. Kulhawy, F. H. "Finite Element Modeling Criteria for Underground Openings in Rock." International Journal of Rock Mechanics, Mining Science & Geomechanical, Abstract, Vol. 11, Pergamon Press, 465-472 (December 1974).

18. Liaw, C. Y., and Chopra, A. K. "Earthquake Response of Axisymmetric Tower Structures Surrounded by Water." A Report to the Office of the Chief Engineers, Dept. of the Army, Washington, D. C. (Oct. 1973).

19. Lysmer, J. L., and Kuhlemeyer, R. L. "Finite Dynamic Model for Infinite Media." Proceedings of the ASCE, EMD, Vol. 95, No. EM4, 859-877 (1969).

20. Moselhi, O. "Finite Element Analysis of Dynamic-Structure Interaction with Some Reference to Underground Nuclear Reactor Containments." M. Eng. Thesis, Memorial University of Newfoundland (1975).

21. Mufti, A. A., Mirza, M. S., McCutcheon, J. O., and Spokowski, R. "A Study of Non-linear Behaviour of Structural Concrete Elements." Symposium on Finite Element Method, McGill University (1970).

22. Nickell, R. E. "Direct Integration Methods in Structural Dynamics." Journal of the Engineering Mechanics Division, Proceedings of the ASCE, 303-317 (April 1973).

23. Obert, L., and Duvall, W. I. "Rock Mechanics and the Design of Structures in Rock." John Wiley & Sons, Inc. (1967).

24. Pao, Y. H., and Mow, C. C. "Diffraction of Elastic Waves and Dynamic Stress Concentrations." Arand Corporation Research Study (1972).

25. Parker, H. W., and Semple, R. M. "Development and Large Scale Testing of Innovative Tunnel Support Systems." Proceedings, North American Rapid Excavation and Tunnelling Conference, American Institute of Mining, Metallurgical and Petroleum Engineers, Chapter 27, 469-497 (1972).

26. Przemieniecki, J. S. "Theory of Matrix Structural Analysis." McGraw Hill Book Company (1968).

27. Reddy, D. V., and Kierans, T. W. "Interaction of Seismic Waves with Underground Nuclear Structures." Proceedings of the Third National Meeting of the Universities Council for Earthquake Engineering Research, University of Michigan, Ann Arbor (May 9-10, 1974).

28. Sigvaldson, O. T., Benson, R. P., and Thompson. "Stress Analysis of Underground Openings in Rock Using the Finite Element Method." Annual Conference of the Engineering Institute of Canada, Halifax (May 1968).

29. Szechy, K. "The Art of Tunnelling." Translated from the Hungarian, Akademiai Kiado, Budapest (1973).

30. Terzaghi, Karl, and Richart, F. E. "Stresses in Rock Around Cavities." Geotechnique - The International Journal of Soil Mechanics, III, No. 2, pp. 57-90 (June 1952).

31. Trollope, D. H. "The Mechanics of Discontinua or Clastic Mechanics." Rock Mechanics in Engineering Practice. Wiley and Sons (1968).

32. Valliappan, S., and Doolan, T. F. "Non-linear Stress Analysis of Reinforced Concrete." Journal of the Structural Division, ASCE, 885-898 (April 1972).

33. Watson, M. B., Kammer, W. A., Langley, N. P., Selzer, L. A., and Beck, R. L. "Underground Nuclear Power Plant Siting." Report No. 6, Cal. Tech. (Sept. 1972).

34. Yu, N. S., and Coates, D. F. "Development and Use of Computer Programmes for Finite Element Analysis." Research Report R. 198, Dept. of Energy, Mines and Resources, Ottawa (July 1969).

35. Zienkiewicz, O. C. "Continuum Mechanics Approach to Rock Problems." Proceedings of the University of Swansea Rock Mechanics Symposium (April 1967).

36. Zienkiewicz, O. C. "The Finite Element Method in Engineering Science." McGraw Hill (1971).

SELECTED BIBLIOGRAPHY

SELECTED BIBLIOGRAPHY

1. Achenbach, J. D. "Wave Propagation in Elastic Solids." North-Holland Publishing Company (1973).

2. Agrawal, P. K. "Comparative Study for Soil-Structure Interaction Effect by the Soil Spring and Finite Element Model." Sargent and Lundy Report, No. SAD-082 (January 1973).

3. Agrawal, P. K., Chu, S. L., and Shah, H. H. "Comparative Study of Soil Spring and Finite Element Models for Seismic Soil-Structure Interaction Analysis of Nuclear Power Plants." Speciality Conference of Structural Design of Nuclear Plant Facilities, ASCE, Vol. 2 (December 1973).

4. Benson, R. P., and Kierans, T. W. "In situ and Induced Stresses at the Churchill Falls Underground Powerhouse, Labrador." Second Congress of the International Society of Rock Mechanics, Belgrade, Yugoslavia (September 1970).

5. Blake, A. "Strength of Underground Cavities." Lawrence Livermore Laboratory, Internal Document ENN 72-59 (1972).

6. Blake, A. "Seismic Protection of Buried Structures." Asilomar Conference 1972, Lawrence Livermore Laboratory, Internal Document ENN 72-150 (1972).

7. Blake, A., Karpenko, V. N., McCauley, E. W., and Walter, C. E. "A Concept for Underground Siting of Nuclear Power Reactors." Lawrence Livermore Laboratory, Report UCRL-51408 (1973).

8. Brekke, T. L., and Glass, C. E. "Some Considerations Related to Underground Siting of Nuclear Power Plants in Rock." Department of Civil Engineering, University of California, Berkeley (March 1973).

9. Chang, C. Y., Nair, K., and Karwoski, W. J. "Finite Element Analysis of Excavation in Rock." Application of the Finite Element Method in Geotechnical Engineering, Proceedings of the Symposium held at Vicksburg, Mississippi, Vol. 2, 457-504 (May 1972).

10. Coates, D. F. "Rock Mechanics Principles." Mines Branch Monograph 874, Department of Energy, Mines and Resources, Ottawa (1967).

11. Costantino, C. J., and Marino, R. L. "Response of Cylindrical Shells Encompassed with Isolation Material to a Plane Pressure Pulse." Technical Report No. AFWL-TR-65-122, IIT Research Institute, Chicago, Illinois (February 1966).

12. Costantino, C. J., Wachowski, A., and Barnwell, V. L. "Finite Element Solution for Wave Propagation in Layered Media Caused by a Nuclear Detonation." Proc. Int. Symposium on Wave Propagation, New Mexico, 59-70 (1967).

13. Costantino, C. J., and Vey, E. "Response of Buried Cylinders Encased in Foam." Proc. ASCE, SMD, 1159-1179 (1969).

14. Dawkins, W. P. "Dynamic Response of a Tunnel Liner-Packing System." Ph.D. Thesis, University of Illinois, Urbana (1969).

15. Dixon, J. D. "Analysis of Tunnel Support Structure with Consideration of Support-Rock Interaction." Report of Investigations 7526, U. S. Dept. of the Interior, Bureau of Mines, Washington (1971).

16. Forrestal, M. J., Reddy, D. V., and Herrmann, G. "Response of a Cylindrical Shell to an Elastic Wave." Journal of the Engineering Mechanics Division, ASCE, EM3, 1-11 (June 1965).

17. Forrestal, M. J. "Transient Response at the Boundaries of a Cylindrical Cavity in an Elastic Medium." Int. J. Solids Structures, Vol. 4, 391-395, Pergamon Press (1968).

18. Ghaboussi, J. "Finite Element for Rock Joints and Interfaces." Journal of the Soil Mechanics and Foundations Division, ASCE, Vol. 99, No. SM10, 833-847 (1973).

19. Ghaboussi, J., and Ranken, R. E. "Tunnel Design Considerations -- Analysis of Medium-Support Interaction." Report No. FRA-ORD & D 75-24, Department of Civil Engineering, University of Illinois, Urbana, Illinois (November 1974).

20. Glass, C. E. "Seismic Considerations in Siting Large Underground Openings in Rock." Ph.D. Thesis, University of California, Berkeley (1974).

21. Hadjian, A. H., and Tsai, N. C. "Soil-Structure Interaction: Continuum or Finite Element?" Bechtel Power Corporation, Los Angeles, California (1974).

22. Humar, J. L., and Wright, E. W. "Numerical Methods in Structural Dynamics." Canadian Journal of Civil Engineering, Vol. 1, 179-193 (1974).

23. Jaeger, J. C., and Cook, N. G. W. "Fundamentals of Rock Mechanics." Methuen & Co. Ltd., (1969).

24. Judd, W. R., and Perloff, W. H. "Predicted and Measured Displacements for Tunnels." ASCE Symposium on Underground Rock Chambers, Phoenix, Arizona, 487-514 (1971).

25. Kierans, T. W., Reddy, D. V., and Heale, D. G. "Dynamic Analysis and Structural Design of Underground Nuclear Reactor Containments."

A paper to be presented at the International Seminar on "Extreme Load Conditions and Limit Analysis Procedures for Structural Reactor Safeguards Structures." (ELCALAP), Berlin (September 1975).

26. Kuhlemeyer, R. L. "Vertical Vibrations of Footings Embedded in Layered Media." Ph.D. Thesis, University of California, Berkeley (1969).

27. Kulhawy, F. H. "Stresses and Displacements Around Openings in Homogeneous Rock." Int. J. Rock Mech. Min. Sci. & Geomech. Abstr., Vol. 12, 43–57, Pergamon Press (1975).

28. Lajtai, E. Z., and Lajtai, V. N. "The Collapse of Cavities." Int. J. Rock Mech. Min. Sci. & Geomech. Abstr., Vol. 12, 81–86, Pergamon Press (1975).

29. McChesney, R. S. "Improved Finite Element Analysis of Nuclear Containment Shell Structures." Paper presented at National Symposium on Computerized Structural Analysis and Design, George Washington University (March 1972).

30. McCreath, D. R. "Layout Considerations for Underground Siting." Course on Continuing Education in Engineering, University of California, Berkeley (November 1973).

31. Murthy, G. K. N., and Reddy, D. V. "Response of Embedded Spherical Shell to a Plane Wave." Nuclear Engineering and Design 5, 426–432 (1967).

32. Paul, S. L. "Interaction of a Plane Elastic Waves With a Cylindrical Cavity." Ph.D. Thesis, University of Illinois, Urbana (1963).

33. Peter, K. H., and Stoykovich, M. "Analysis and Design of Nuclear Power Plant Structures." Speciality Conference on Structural Design for Nuclear Plant Facilities, ASCE, Vol. 2 (December 1973).

34. Rizzo, P. C. "Seismological/Geologic Criteria and Considerations for Siting Surface and Underground Nuclear Plants." Specialist Meeting, Antiseismic Design of Nuclear Power Plants, Pisa, Italy (October 1972).

35. Seed, B., Lysmer, J., and Hwang, R. "Soil-Structure Interaction Analyses for Seismic Response." Journal of the Geotechnical Engineering Division, ASCE, GT5, 439–457 (May 1975).

36. Setlur, A. V., Khanna, J. K., and Valthur, M. "A New Approach to Soil-Structure Interaction Problems." Speciality Conference on Structural Design of Nuclear Plant Facilities, ASCE, Vol. 2 (December 1973).

37. Swiger, W. F. "Can We Place Nuclear Power Plants Underground." Presented at Geological Society of America, Washington, D. C. (November 1971).

38. Tsai, N. C. "A Discussion of Agrawal Paper: Comparative Study for Soil-Structure Interaction by the Soil Spring and Finite Element Model." Bechtal Power Corporation, San Francisco, California (October 1973).

39. "Underground Nuclear Power Plants -- A Preliminary Evaluation." United Engineers & Construction Inc. and Acres American Incorporated, UEC-UNP-710701 (July 1971).

40. Waas, G., and Lysmer, J. "Vibrations of Footing Embedded in Layered Media." Application of the Finite Element Method in Geotechnical Engineering, Proceedings of the Symposium Held at Vicksburg, Mississippi, Vol. 2, 581-604 (May 1972).

41. Whitman, R. V. "Basic Concepts and Important Problems." Proceedings of the Seminar on Seismic Design of Nuclear Power Plants. Ed. R. J. Hansen, M.I.T. Press, U.S.A., 1-68 (1970).

42. Whitman, R. V. "Soil-Structure Interaction." Proc. of the Seminar on Seismic Design of Nuclear Power Plants. Ed. R. J. Hansen, M.I.T., U.S.A., 345-369 (1970).

43. Whitman, R. V. "Analysis of Dynamic Soil-Structure Interaction for Nuclear Plants." Notes for Panel Discussion in the ASCE Speciality Conference, Chicago (December 1973).

44. Wood, V. D., and Van Eysvyk, R. J. "Case History of Williams Pre-stressable Hollow Groutable Rebar Spin-Lock Rock Bolts Used in Underground Diversion Tunnels at Churchill Falls." Proceedings of the Eleventh Annual Engineering Geology and Soils Engineering Symposium, Held at Pocatello, Idaho (April 4, 5 and 6, 1973).

45. Yoshihara, T., Robinson, A. R., and Merrit, J. L. "Interaction of Plane Elastic Waves With an Elastic Cylindrical Shell," Civil Engineering Studies, Structural Research Series No. 261, University of Illinois (1963).

46. Zeevaert, L. "Foundation Engineering for Difficult Subsoil Conditions." Van Nostrand Reinhold (1973).

APPENDIX A

APPENDIX A

1. a) <u>Bar Element Stiffness Matrix</u>
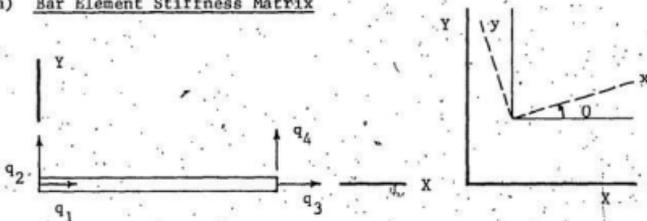
$[K_e]_{4\times4}$ Element stiffness matrix in local coordinates

$$[K_e]_{4\times4} = \begin{bmatrix} +1 & 0 & -1 & 0 \\ 0 & 0 & 0 & 0 \\ -1 & 0 & 1 & 0 \\ 0 & 0 & 0 & 0 \end{bmatrix}$$

b) $[R]_{4\times4}$ <u>Transformation Matrix</u>

$$[R]_{4\times4} = \begin{bmatrix} C & -S & 0 & 0 \\ S & C & 0 & 0 \\ 0 & 0 & C & -S \\ 0 & 0 & S & C \end{bmatrix} \qquad \begin{array}{l} C = \text{Cos } \theta \\ S = \text{Sin } \theta \end{array}$$

c) $[K]_{4\times4}$ <u>Element Stiffness Matrix in Global Coordinates</u>

$$[K]_{4\times4} = [R][K_e][R]^T$$

$$[K]_{4\times4} = \begin{bmatrix} c^2 & sc & -c^2 & -sc \\ cs & s^2 & -cs & -s^2 \\ -c^2 & -sc & c^2 & sc \\ -cs & -s^2 & cs & s^2 \end{bmatrix}$$

114

2. Frame Element Stiffness Matrix
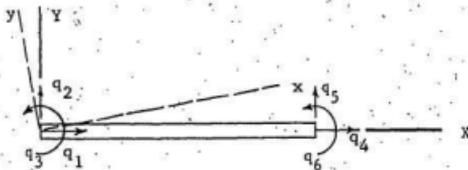
$$
[K_e]_{6 \times 6} = \frac{EI}{l^3}
\begin{bmatrix}
\dfrac{Al^2}{I} & & & & & \\
0 & 12 & & & \text{Symmetrical} & \\
0 & 6l & 4l^2 & & & \\
-\dfrac{Al^2}{I} & 0 & 0 & \dfrac{Al^2}{I} & & \\
0 & -12 & -6l & 0 & 12 & \\
0 & 6l & 2l^2 & 0 & -6l & 4l^2
\end{bmatrix}
$$

$$
[R]_{6 \times 6} =
\begin{bmatrix}
l_x & m_x & 0 & 0 & 0 & 0 \\
l_y & m_y & 0 & 0 & 0 & 0 \\
0 & 0 & 1 & 0 & 0 & 0 \\
0 & 0 & 0 & l_x & m_x & 0 \\
0 & 0 & 0 & l_y & m_y & 0 \\
0 & 0 & 0 & 0 & 0 & 1
\end{bmatrix}
$$

l_x, m_x, l_y and m_y are the direction cosines of the new axes x and y relative to the axes X and Y.

$$[K] = [R][K_e][R]^T$$

This matrix multiplication is done within the computer programme.